SYNTHESIS OF CHITOSAN/ACTIVATED CARBON COMPOSITE FOR ADSORPTION OF BRILLIANT BLACK BN DYE FROM AQUEOUS SOLUTION

MUHAMMAD AZRIE BIN RAZAM

UNIVERSITI SAINS MALAYSIA

2021

SYNTHESIS OF CHITOSAN/ACTIVATED CARBON COMPOSITE FOR

ADSORPTION OF BRILLIANT BLACK BN DYE FROM AQUEOUS SOLUTION

by

MUHAMMAD AZRIE BIN RAZAM

Project proposal submitted in partial fulfillment of the requirement for the degree of

Bachelor of Chemical Engineering

2021

ACKNOWLODGEMENT

TABLE OF CONTENTS

LIST OF TABLES

LIST OF FIGURES

LIST OF SYMBOLS

	Symbols	Unit
a_t	Binding equilibrium constant	L/g
B	Heat of adsorption constant	J/mol
b_T	Temkin isotherm constant	-
C_e	Equilibrium adsorbate concentration	mg/L
C_o	Adsorbate concentration at initial	mg/L
C_t	Adsorbate concentration at time, t	mg/L
k_1	Pseudo-first order sorption rate constant	1/hr
k_2	Pseudo-second order sorption rate constant	g/hr.mg
K_F	Freundlich constant related to capacity	$mg/g(L/mg)^{1/n}$
K_L	Langmuir adsorption constant	L/mg
n_F	Freundlich constant related to adsorption intensity	-
PFO	Pseudo-first-order kinetic model	-
PSO	Pseudo-second-order kinetic model	-
q_e	Equilibrium adsorption capacity	mg/g
q_m	Maximum adsorption capacity of adsorbent	mg/g
q_t	Adsorption capacity at time, t	mg/g
R	Gas constant	8.314 J/mol K
R^2	Coefficient of determination	-
R_L	Coefficient of determination	-
t	Time	min

T	Absolute solution temperature	K
V	Dye solution volume	L
W	Mass of adsorbent	g

LIST OF ABBREVIATIONS

AA	Acetic acid
AC	Activated carbon
BB	Brilliant Black BN dye
CS	Chitosan
CS/AC	Chitosan/activated carbon
DD	Degree of deacetylation
DI	Deionized water
EtOH	Ethanol
IUPAC	International Union of Pure and Applied Chemistry
MOF	Metal organic frameworks
NaOH	Sodium hydroxide
SDGs	Sustainable Development Goals
UV	Ultraviolet

SINTESIS KITOSAN/KARBON TERAKTIF UNTUK PENYERAPAN PEWARNA

BRILLIANT BN HITAM DARIPADA LARUTAN AKUEUS

ABSTRAK

Pencemaran air adalah salah satu masalah terbesar yang boleh membahayakan ekosistem akuatik dan tamadun manusia jika ia tidak ditangani dengan sewajarnya. Salah satu faktor yang menyumbang kepada pencemaran air ialah pencemaran bahan pewarna yang disebabkan oleh sifat kestabilannya yang tinggi terhadap cahaya, suhu, detergen, bahan kimia, pelunturan, dan tidak terbiodegradasi seperti pewarna Brilliant black BN (BB). Tujuan kajian ini adalah untuk mensintesis kitosan (CS) dan kitosan/karbon teraktif (CS/AC) komposit penjerap dengan menggunakan kaedah tuangan larutan dan untuk menyiasat keberkesanan prestasi penjerap ke atas penyingkiran pewarna BB daripada larutan akueus. Tiga parameter iaitu dos penjerap, kepekatan pewarna awal dan masa sentuhan perlu dikenal pasti melalui eksperimen mod kelompok proses penjerapan. Kecekapan penyingkiran CS/AC didapati lebih tinggi sedikit iaitu 97.18 % jika dibandingkan dengan CS 96.14 % pada kepekatan pewarna BB awal 40 mg/L dan dos penjerap 2.5 g. Data keseimbangan eksperimen dikaji menggunakan isoterma Langmuir, Freundlich dan Temkin. Model Temkin didapati paling sesuai untuk menggambarkan penyingkiran pewarna BB. Tambahan pula, model kinetik urutan pseudo-pertama paling sesuai untuk kajian kinetik penjerapan pada filem komposit. Oleh itu, filem penjerap komposit CS dan CS/AC mempunyai keupayaan untuk mengeluarkan pewarna BB daripada air sisa kumbahan.

SYNTHESIS OF CHITOSAN/ACTIVATED CARBON COMPOSITE FOR ADSORPTION OF BRILLIANT BLACK BN DYE FROM AQUEOUS SOLUTION

ABSTRAC

Water pollution is one of the biggest disasters that can endangered the aquatic ecosystem and human civilization if it did not been treated accordingly. One of the factors that contribute to the water pollution is by the contamination of dye due to it is high stability properties towards light, temperature, detergents, chemicals, bleaching, perspiration and non-biodegradable such as the Brilliant black BN (BB) dye. The purpose of this study is to synthesis the chitosan (CS) and chitosan/activated carbon (CS/AC) composite adsorbent by using solution casting method and to investigate the performance of the resultant adsorbents on removal of BB dye from aqueous solution. Three parameters such as adsorbent dosage, initial dye concentration and contact time were to be identified through batch mode adsorption experiment. The removal efficiency of CS/AC is found to be slightly higher at 97.18 % while CS is 96.14 % at 40 mg/L initial BB dye concentration and 2.5 g adsorbent dosage. The experimental equilibrium data were studied using Langmuir, Freundlich and Temkin isotherms. The Temkin model is found the best to describe the removal of BB dye. Furthermore, pseudo-first order (PFO) kinetic models best fit kinetic studies of adsorption onto composite films. Hence, the CS and CS/AC composite adsorbent films have a capability to remove BB dyes from the wastewater.

CHAPTER ONE

INTRODUCTION

The food industry has grown globally and this industry commonly used dyes to give colors to food product to make it more attractive. Many different types of food dyes are available in the food industry. However, the two main famous dye types are natural and synthetic dyes. Natural dyes are mainly made by extracting natural pigments from plants, animals, and minerals, while synthetic fabric dyes are synthesis in a laboratory or factory.

1.1   Research background

In terms of both volume and effluent composition, wastewater generated from food industries is categorized as most polluting plants compared to the other industrial sectors (Patients et al., 2012). Furthermore, increased demand for food products, causing more dyes needed during the food product manufacturing that eventually contributed to dye wastewater. This situation has become one of the major sources of pollution in present times. Because of their thermal resistant and photo stability is high to avoid biodegradation, dyes can stay in the environment for long a term.

In late '90s, water purification processes such as sedimentation and equalization were used for dye removal since there was no limit to effluent for industrial discharge ordered by the government (Bhatt et al., 2000). Improvements were made after the establishment of the implementation of the dye effluent released standard. This improvement method is made in order to discharge the dye in a more effect way (Mezohegyi et al., 2012). Following that, a

system of wastewater treatment consists of pretreatment, primary treatment, chemical or physical separation treatment, secondary treatment, tertiary treatment, sludge and disposal were used. This dye removal system was applied by some industries but it was stopped due to its uneconomically operation and maintenance cost (Adegoke and Bello, 2015). Current methods to remove dye can be separated into several categories, namely the biological, chemical, and physical methods (Tang et al., 2018). Physical dye removal is the most popular among the three methods. Adsorption emerged as one of the preferred removal techniques due to its ability to remove almost any type of pollutants (Crini, 2006a).

One of the most effective and genuine physicochemical treatments has been adsorption by activated carbon adsorbent. Chemicals is used to change the physical characteristics of colloidal particles, making them easily to coagulable for further treatment and filtration, is known as physicochemical treatment. For over a century, these treatment methods have been used in conjunction with biological treatment methods. AC is famous with its porous structure that consist of high surface area and its great adsorption capacities towards pollutants. A wide resources of cheap biomass materials, such as bagasse pith, wood, maize cob and peat, are being studied as potential substitutes for producing activated carbon for removal of dyes (Malik, 2004). Commercial activated carbons are refined because they are designed for a wide range of applications.

CS is a biological based polymer that is chemically nontoxic, cationic properties and biodegradable polysaccharide (Riva et al., 2011). CS is synthesis from the alkaline deacetylation of chitin (Jin Li, 2013). Hydrolysis of acetyl groups inside chitins are converted to free amine groups. The degree of deacetylation (DD) or the ratio of de-acetylated to acetylated units is determine in this step. DD is affected by operating temperature, time, and

2

concentration of sodium hydroxide used for deacetylation (John Kasongo et al., 2020). A high degree of DD is typically caused by a high concentration of amino groups, which increases the adsorption capacity of the CS via protonation of the amino group (Piccin et al., 2009). The adsorption capacity of CS is affected by the degree of DD. Due to hydrogen bonds between its molecules, CS is not soluble in alkaline solutions, organic solvents and water. CS is soluble in acidic solution due to protonation of its amine groups (Aranaz et al., 2009). This describe that CS have potential to adsorb pollutions such as dyes and heavy metals (Peng et al., 2013). However, some drawbacks such as acidic solubility and poor mechanical strength can influence the performance of this adsorbent in the adsorption process.

The sustainable development goals (SDGs) are intended to ensure a sustainable future for all living things on earth. This project is related to SDGs Goal 6, 12 and 14. SDG Goal 6 is about clean water and sanitation that ensure a fully access of clean water and sanitation for all. Goal 12 is accountable for production and consumption while Goal 14 aims to conserve and sustainably manage maritime resources. In this project, Goal 6 and 14 are committed to achieve sustainable development by the adsorption technique. The adsorption process is one of the treatments that are commonly used to removed pollutant from the water. This method is simple, save and economical that can provide clean water for all organism especially aquatic life. In this study, Goal 12 is related to the material used for the adsorption process. Polymer nanocomposite is one of the options for the adsorption technique. The polymer use is CS that comes from crustaceans which is protein-rich sources that are produced in millions of tons worldwide, and these valuable food sources contain non-edible parts in the form of shells that constitute more than half of their body mass which is called chitin. CS is a valuable

product that can be a suitable adsorbent used in the wastewater treatment industries. Compared to the other conventional adsorbent, CS adsorbent is more flexible that can be in the form of film, beads, membrane and flakes. The CS adsorbent can also be combined with a variety of other additives to form composites or hybrids. Goal 12 can be achieve by consuming the crustacean waste to produce adsorbent for wastewater treatment.

1.2   Problem statement

From an environmental point of view, the dye effluents discharge from manufacturing or consuming units into the water bodies can threatened the water quality. 2 % of dyes are approximately lost during production, and about 15% of dyes are discharged as effluent during the dye was applied (Husain, 2006). It causes serious health problems for all organism that consume the affected, mainly aquatic life. Due to their stability to light, temperature, detergents, chemicals and bleaching agents is high, most of these dyes escape the conventional wastewater treatment system and remain in the environment (Rodríguez Couto, 2009). The removal of dye by the adsorption method is the most preferred technique because of its remarkable ability to get rid of almost any type of dye in the solution (Crini, 2006a). Due to low cost of AC adsorbent, it has become a typical adsorbent for wastewater treatment. The adsorptive properties of AC will gradually deteriorate after continuous dye removal (Wawrzkiewicz, 2012). AC will not have limitless adsorption capacity as the pores have become saturated with the dye molecules. Other than that, the AC hardly to be reactivated (Chowdhury, 2013). The major drawback of adsorbents such as AC and carbon nanotubes is during complete separating process from aqueous solution by filtration and centrifugation methods due to tiny in size and secondary turbidity (Thinh et al., 2013). Other

4

adsorbent that can be used to adsorb the dye is the CS adsorbent. Although CS is an effective adsorbent for a variety of pollutants. However, CS suffers from poor mechanical properties and thermal stability. Therefore, the CS need to be combined with a variety additive to form a strong composites or hybrids. Cellulose (Wittmar et al., 2020), starch (Chen et al., 2020), bentonite (Fonseca, 2021), zeolites (Lin and Zhan, 2012), and metal organic frameworks (MOFs) (Zhao et al., 2020) are among these additives. Since AC is the cheap and effective adsorbent, thus, the current study will focus on incorporating of AC into CS to form a composite adsorbent for Brilliant black BN (BB) dye removal.

1.3   Objectives

1. To synthesize the CS and CS/AC composite films type adsorbent using solution casting method for adsorption process.

2. To understand the effect of adsorbent dosage, initial dye concentration and contact time on adsorption of BB dye.

3. To investigate the adsorption isotherm and kinetic of the CS/AC composite film adsorbent.

CHAPTER TWO

LITERATURE REVIEW

Dyes are substances that change a substrate's crystal structure to produce color (Bafana et al., 2011). Food, textile, plastics, and paper industries use these substances for their own application (Carneiro et al., 2007). Dye solutions can form covalent bonds, physical adsorption, or mechanical retention with compatible surfaces (Bafana et al., 2011). Dyes contain chromophores, which give dyes their color. These chromophore-containing centers are azo, anthraquinone, methine, nitro, aril methane, carbonyl, etc. Auxochromes, which are amine, carboxyl, sulfonate, and hydroxyl, are electron-withdrawing or -donating substituents used to generate or intensify chromophore color (Prasad and Rao, 2010).

2.1   Classification of dyes

The foundation for classifying dyes substances is their chemical structures, which influence their colors, qualities, and applications. A more reasonable classification of dyes and their chemical structure is by placing chemically similar compounds close together. Within each major category, dyes can be classified according to chromophore and substituent differences. Table 2.1 shows the general group of dyes.

Table 2.1: Group of dyes application method and its chemical type (Kiernan, 2001)

Class	Application method	Chemical type	Example
Acid	Colored anions applied to wool, nylon, silk at low pH	Azo, Anthraquinone, Premetalized and Triphenylmethane	Acid blue 45
Azoic	The reaction between a diazonium salt (azoic diazo component) and naphthol generates insoluble azo dyes in the substrate (azoic coupling component).	Monoazo, Diazo and Polyazo	Methyl orange, Methyl red, Congo red
Basic	Traditionally, colored cations were also used on proteinaceous fibers and cotton treated with tannic acid.	Cyanine, hemocyanin, diazahemicyanine, diphenylmethane, triarylmethane, azo, azine, xanthene, acridine, oxazine, anthraquinone	Methylene Blue, Toluidine Blue, Thionine, and Crystal Violet.
Food	Substances used to color foodstuffs	Beta-carotene, Anthocyanin, Carminic Acid	Brilliant Blue FCF, Allura Red AC

Table 2.1: Continued

Sulfur	Heating aromatic amines and phenols make cheap polymeric dyes with sulfur or sodium polysulfide.	Indeterminate structures	Sulphur Black 1
Reactive	Colored compounds with side chains that react with the substrate to form covalent bonds; used to provide very fast (resistant) dyeing of cellulose.	Azo, anthraquinone, phthalocyanine, formazan, oxazine, basic	Reactive Blue 3
Vat	Utilized primarily on cotton as a soluble compound that is oxidized into an insoluble, fully colored form of the dye.	Anthraquinone (including polycyclic quinones), indigoids	Vat Blue 4

2.2   Brilliant Black BN Dye

Brilliant black BN (BB) is an azo dye with the molecular formula 4-acetamido-5-hydroxy-6-[7-sulfonato-4-(4-sulfonatophenylazo)-1-naphtylazo]   naphthalene   1,7-disulfonate. BB has the chemical formula $C_{28}H_{17}N_5Na_4O_{14}S_4$ and the molecular weight of 867.68 g/mol. Black PN, Food Black 1, Naphthol Black, and C.I. Food Black 1 are the alternative names for BB. BB is a tetrasodium salt that is water-soluble. It resembles a solid, a powder, or granules (Macioszek and Kononowicz, 2004) BB's structural formula is depicted in Figure 2.1.
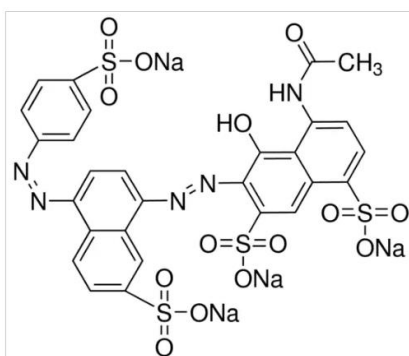
Figure 2.1: Chemical Structure of Brilliant Black BN dye

BB is utilized primarily in food decorations and coatings, desserts, sweets, ice cream, mustard, red fruit jams, soft drinks, flavored milk drinks, fish paste, and other foods. The maximum amount of BB permitted in food is 100 mg/L (or kg^{-1}) of the product's weight (100 g mL^{-1}) as approved by the Food and Drug Administration (FAO, 2014). It appears to cause allergic or intolerance reactions, particularly in aspirin-sensitive individuals. As a histamine releaser, it may exacerbate asthma symptoms. Therefore, the necessary measures must be taken to eliminate BB dye from wastewater.

2.3   Method of dye removal

Elimination of dye from the industrial effluents are very important to ensure the environment are not polluted. Some dyes can be toxic that can cause harm to the aquatic ecosystem if it does not handle properly. There are various types of method to remove dye that mainly categorized in the biological, chemical and physical treatment.

Biological dye removal is the most common method in most nations. The conventional method uses aerobic and anaerobic processes to treat dye effluents before release. This method was chosen because it's cheap and easy to use (Robinson et al., 2001). The conventional method only treats wastewater's chemical oxygen demand, but not dyes or toxins. Traditional biological dye removal methods include microbial biomass adsorption, algae degradation, enzyme degradation, and fungal, microbial, pure, and mixed cultures. Living organisms are used in biological dye removal. This method must be used carefully and ethically. Enzymes are popular for removing dye. Biological dye removal is the cheapest and safest method (Pan et al., 2017). However, the main drawback is the organism's growth rate. In biological dye removal processes, system instability is common because the growth rate and reactions are hard to predict.

Chemical dye removal procedures include advanced oxidation, electrochemical destruction, dye removal via the Fenton reaction, oxidation reduction, ozonation, photochemical and ultraviolet irradiation. Except for electrochemical degradation, most chemical dye removal procedures are expensive than biological and physical methods. Chemical dye removal is not commercially viable since it needs specialist equipment and a lot of electricity (Cui et al., 2012). Chemical dye removal equipment requires a lot of electricity. High chemical and reagent usage is another concern (Crini, 2006b). The

elimination of chemical dyes causes harmful secondary pollutants, posing a disposal problem (Wang et al., 2018).

Physical dye removal uses mass transfer concept. Physical dye removal techniques include adsorption, coagulation, ion exchange, irradiation, membrane filtration, nanofiltration, ultrafiltration, and reverse osmosis. Table 2.2 shows the advantages and disadvantages of the physical dye removal methods. Physical dye removal techniques are the most common. Simple and effective, these methods are popular. This method uses less chemicals than biological and chemical dye removal (Khan et al., 2018). This method doesn't involve living organisms and is therefore more reliable.

Table 2.2: Advantages and disadvantages of physical dye removal methods (Katheresan et al., 2018)

Method	Description	Advantages	Disadvantages
Adsorption	Adsorbents made from materials with a high adsorption capacity to absorb dye molecules.	Excellent method for removing a wide variety of dyes.	Re-generable adsorbent. Absorbents can be expensive.
Coagulation and flocculation	Dye wastewater is treated with coagulation/flocculation agents to agglomerate dye particles. Filtration removes aggregates.	Cheap. Method with a high degree of reliability. Only compatible with disperse, sulphur, and vat dye effluents.	Massive amounts of concentrated sludge are produced. Not suitable for effluents containing acid, azo, basic, or reactive dyes.
Ion exchange	Reversible chemical process where dye wastewater ions swap positions with solid-surface ions.	Regenerable Good dye remover. Creates high-quality water.	Effective to a limited number of dyes Effective against a small number of dyes
Membrane filtration	A membrane separates dye from wastewater.	Effective for recovering and reusing water.	Start-up costs high. Membrane fouling simply occur It produces sludge. Not suitable for dye elimination
Nano filtration and ultra-filtration	Dye-contaminated wastewater is filtered by a membrane. A membrane separates dye from wastewater.	Can remove any type of dye High cost. Expensive dye remover	Intensive energy usage. Dye molecules continually obstruct the pores of membranes.
Reverse osmosis	A pressure-driven system that pushes water across a thin membrane, separating pollutants from water.	Common method of water recycling Effective at decolorizing and desalting numerous dyes. Produces pure and clean water.	Costly. Requires high pressure

2.3   Adsorption method

Adsorption is a mass transfer mechanism between gas-liquid, gas-solid, liquid-liquid, and liquid-solid phases (Yagub et al., 2014). Adsorption is a high-efficiency water purification separation technique. Adsorption is a non-reactive process that concentrates a gas or liquid on a solid surface (Nguyen and Juang, 2013). Adsorbate is the adsorbed substance; adsorbent is the adsorbing substance. Chemical and physical sorption are adsorption procedures (Tang et al., 2018). With a few exceptions, physisorption is used for adsorption. In physisorption, dipole-dipole, hydrogen bonds, and polar bonds can also ensure adsorption in most solid-liquid systems, producing a colorless treated solution from solid adsorbent and dye effluent. The adsorbent captures dye particles from the dye solution. The system is in dynamic equilibrium when all dye molecules are adsorbed. Adsorption removes dye effectively without additional equipment (Wang et al., 2011). Adsorption is usually used to decolorize dye effluents. Porous materials are best for dye adsorption (Ganiyu et al., 2017). The lack of toxic byproducts makes adsorption excellent for pollution management (Rafatullah et al., 2010). Correctly built adsorption systems create high-quality treated effluents.

2.3.1   Physisorption and chemisorption

Physisorption (or physical adsorption) involves intermolecular forces (van der Waals forces) similar to those responsible for the imperfection of actual gases and the condensation of vapors, and the electronic orbital patterns of the species involved do not change. The general phenomena that occur in solid or liquid systems helps identify physisorption. Geometrical or electrical features of the adsorbent and/or adsorptive may cause unique

molecular interactions (IUPAC, 1979). Minimal evidence implies adsorbent, and adsorbate electronic states are disturbed. Adsorption and desorption have no effect on the fluid's chemical composition since adsorbed species are chemically equivalent to fluid species. Typically, adsorbate-adsorbent interaction energy is larger than adsorptive condensation energy. Physical adsorption from gas requires no activation energy. Rate-determining transport systems can cause sluggish, temperature-dependent equilibration. Physical adsorption increases with gas pressure and decreases with temperature in low-pressure solid or gas systems. A system's metastable equilibrium may display hysteresis. Under the right pressure and temperature, more gas molecules can be adsorbed than surface molecules (multilayer adsorption or filling of micropores).

Chemisorption involves valence forces of the same type as those in chemical compound synthesis. Chemisorption and physisorption are similar to chemical and physical interactions in general. Chemisorption is characterized by chemical specificity. Physical approaches can detect electronic state changes (e.g., U.V., infrared or microwave spectroscopy, electrical conductivity, magnetic susceptibility). Chemisorption may not be reversible if surface dissociation or reaction modifies the adsorptive(s) so that the original species cannot be recovered upon desorption. Chemisorption has the same energy as a solid-fluid chemical reaction; therefore, it can be exothermic or endothermic, with minor to large energy changes. When the activation energy for adsorption is high, activation energy plays a role in chemisorption (activated adsorption). In practice, balance may be slow or nonexistent. In the adsorption of gases by solids, the extent of adsorption at a constant gas pressure after a certain period may increase as temperature rises. When the activation energy for desorption is high, chemisorbed species may only be removed from a surface under

14

extreme temperature, vacuum, or chemical treatment. Valence bonds bind adsorbed molecules to the surface, so they occupy specific locations. chemisorbed molecules create a single layer (monolayer adsorption).

2.4   Chitosan/and activated carbon

Chitosan is generated by deacetylating chitin. Chitosan is biodegradable, biocompatible, hydrophilic, and absorbent. Chitosan's reactive functional groups (hydroxyl, -OH; amino, -NH2) can bind anionic dyes and metal ions. Covalently bound -OH groups form hydroxyl (alcohol) groups. The hydroxyl group in biological compounds is often attached to carbon. Since oxygen is more electronegative than hydrogen or carbon, covalent bond electrons spend longer time surrounding it. The hydroxyl group's O-H and O-C bonds are polar covalent bonds. The amino group is formed by single bonds between nitrogen and hydrogen. An amine contains an amino group. Nitrogen, like oxygen, is more electronegative than carbon and hydrogen. Since amino groups can act as bases, the nitrogen atom can connect with a fourth hydrogen atom. The nitrogen atom gains a positive charge and can form ionic connections. Due to its high amino and hydroxyl functional group content and low toxicity, chitosan is a useful biopolymer for eliminating a range of contaminants from water (Kakavandi et al., 2014). Solubility in acidic aqueous solutions gives a hydrophilic, biocompatible, and ecologically benign polymer that can be utilized to make membranes, adsorbents, and coatings (Jana et al., 2011).

Activated carbon is a high-surface-area adsorbent that has several uses. This removes organic and inorganic pollutants from water (Ai and Jiang, 2010). Depending on how it's made, activated carbon has primary particles with a few to 100 nm diameter. Activated

carbon aggregates are 200 to 1000 nm in size, while agglomerates are 103 to 106 nm (Donnet, 1995). Table 2.3 compares chitosan nanocomposite adsorption efficiencies.

Table 2.3: Comparison of various chitosan nanocomposite with their adsorption efficiency

Polymer nanocomposite	Dye	Adsorption Efficiency	Reference
Chitosan-Fe_3O_4 (Hollow fiber)	Reactive Blue 19	89.4%	(Seyed Dorraji et al., 2015)
Chitosan-cellulose nanofiber (film)	Methyl orange	96.28%	(Huo et al., 2021)
Chitosan-bentonite	Weak acid scarlet	85%	(Guo et al., 2012)
Chitosan-activated carbon	Methylene Blue	99.45%	(Chang and Chen, 2005)
Chitosan/Polyvinyl Alcohol/zeolitic imidazolate framework	Malachite Green	84.55%	(Khajavian et al., 2020)

2.5   Adsorption isotherm

Adsorption isotherm is an empirical relationship used to predict the maximum amount of solute that an adsorbent can absorb (Desta, 2013). It depicts the distribution of an adsorbable solute between the liquid and solid phases at various equilibrium concentrations (Ng et al., 2002). Langmuir, Freundlich, and Temkin are the three well-known isotherms (Ahmad et al., 2015).

2.5.1 Langmuir isotherm

This model posits that intermolecular forces diminish fast with increasing distance and can therefore be used to forecast the presence of monolayer adsorbate coverage on the adsorbent's outer surface. The linear form of the Langmuir isotherm equation (Langmuir, 1918) is given by:

$$\frac{1}{q_e} = \frac{1}{q_m} + \frac{1}{q_m K_L C_e} \qquad \text{[Equation 2.1]}$$

where:

C_e Equilibrium adsorbate concentration (mg/L)

K_L Langmuir adsorption constant (L/mg)

q_e Equilibrium adsorption capacity (mg/g)

q_m Maximum adsorption capacity of adsorbent (mg/g)

The constant values are derived from the intercept and slope of the linear plot of $\frac{1}{q_e}$ against $\frac{1}{C_e}$. The fundamental properties of the Langmuir equation can be described in terms of the dimensionless separation factor, R_L, which is defined as follows:

$$R_L = \frac{1}{(1 + K_L C_0)} \qquad \text{[Equation 2.2]}$$

where:

C_0 Highest adsorbate concentration at initial (mg/L)

R_L value means adsorption is unfavorable ($R_L > 1$), linear ($R_L = 1$), irreversible ($R_L = 0$) and favorable ($0 < R_L < 1$)

2.5.2 Freundlich isotherm

The Freundlich model is an empirical equation based on the adsorption of heterogeneous surfaces or surfaces with varied site affinities. The assumption is that the stronger binding sites are occupied first, and that the binding strength diminishes as site occupancy increases. The formulation of the Freundlich isotherm (Freundlich, 1907) is as follows:

$$\log q_e = \log K_F + \left(\frac{1}{n_F}\right) \log C_e \qquad \text{[Equation 2.3]}$$

where:

C_e Equilibrium adsorbate concentration (mg/L)

K_F Freundlich constant related with capacity $(\text{mg/g}(\text{L/mg})^{1/n})$

q_e Equilibrium adsorption capacity (mg/g)

n_F Freundlich constant related with adsorption intensity (mg/g)

The constant values are derived from the intercept and slope of the linear plot of $(\log q_e)$ against $(\log C_e)$. If n_F constant is greater than 1 meaning the experimental data is favourable.

2.5.3 Temkin isotherm

Included in the Temkin isotherm is a component that explicitly accounts for adsorbent–adsorbate interactions. This model implies that adsorbent-adsorbate interactions reduce the heat of adsorption of all molecules in a layer linearly with increasing coverage. Following is the formulation of the Temkin model (Temkin, M. and Pyzhev, 1940).

$$q_e = B \ln a_t + B \ln C_e \qquad \text{[Equation 2.4]}$$

where B is RT/bt

at   Heat of adsorption constant (L/g)

B   Heat of adsorption constant (J/mol)

b_T Temkin isotherm constant

C_e Equilibrium adsorbate concentration (mg/L)

q_e Equilibrium adsorption capacity (mg/g)

R   Gas constant = 8.314 J/mol K

T   Absolute solution temperature (K)

The constant values are derived from the intercept and slope of the linear plot of q_e against C_e

2.6 Adsorption kinetic

Adsorption kinetics explains the rate of retention or release of a solute from an aqueous environment to a solid-phase contact when the adsorbent dose, temperature, and pH are held constant. Using pseudo-first order (PFO) and pseudo-second order (PSO) kinetic models, the adsorption mechanism of dyes on the adsorbent is analyzed.

2.6.1 PFO kinetic model

The PFO model is also known as Lagergren model that describes the adsorption of solute onto adsorbent. The equation is shown as (Achparaki et al., 2012):

$$\frac{dq_t}{dt} = k_1(q_e - q_t)$$
        [Equation 2.5]

where:

k_1 rate constant per hour (1/hr)

q_e Equilibrium adsorption capacity (mg/g)

q_t Adsorption capacity at time, t (mg/g)

The integral of Equation 2.5 from t = 0 to t = t and qt = 0 and qt = qt yields a linear expression of PFO model is shown in Equation 2.6

$$ln(q_e - q_t) = \; lnq_e - k_1 t \qquad\qquad \text{[Equation 2.6]}$$

The value of k_1 is determined by plotting $ln(q_e - q_t)$ against t.

2.6.2   PSO kinetic model

According to the PSO model, the rate of solute adsorption on an adsorbent is proportional to the number of accessible sites. The reaction rate is dependent on the amount of solute on the surface of the adsorbent, while the driving force $(q_e - q_t)$ is proportional to the number of active sites available on the adsorbent (Tan and Hameed, 2017). The curvilinear form of the PSO model is illustrated by Equation 2.7:

$$\frac{dq_t}{dt} = \; k_2(q_e - q_t)^2 \qquad\qquad \text{[Equation 2.7]}$$

where:

k_2 rate constant for pseudo second order model (g/hr.mg)

q_e Equilibrium adsorption capacity (mg/g)

q_t Adsorption capacity at time, t (mg/g)

Applying the integral limit for t = 0 to t = t, and qt = 0 and qt = qt with the linearization of

the PSO model, Equation 2.8 is obtained:

$$\frac{t}{q_t} = \frac{1}{k_2 q_e{}^2} + \frac{1}{q_e} t$$

[Equation 2.8]

The value of k_2 is determined by plotting $\frac{t}{q_t}$ against t.

CHAPTER THREE

METHODOLOGY

In this chapter, the information on chemicals used and the experimental work on the synthesis of CS/AC composite and the adsorption of BB dye are described. The experimental work comprises the synthesis of adsorbent, optimization of adsorbent, adsorption efficiency, adsorption isotherm and adsorption kinetic study.

3.1   Flow of experiment work

The overall flow of the experimental work. Figure 3.1 depicts the flow diagram of the experimental work including synthesis of CS/AC films, batch experimental, adsorption isotherm and adsorption kinetics studies.

```
┌─────────────────────────────────────────────┐
│          Preparation of CS/AC solution        │
└─────────────────────────────────────────────┘
                      │
                      ▼
┌─────────────────────────────────────────────┐
│ Solution casting and treatment of CS/AC film adsorbent │
└─────────────────────────────────────────────┘
                      │
                      ▼
┌─────────────────────────────────────────────┐
│           Batch Experimental Studies:         │
│         a) Effect of adsorbent dosage         │
│       b) Effect of initial dye concentration  │
│          c) Effect of contact time            │
└─────────────────────────────────────────────┘
          │                        │
          ▼                        ▼
┌───────────────────┐    ┌───────────────────┐
│ Adsorption Isotherm│    │  Kinetic Studies  │
└───────────────────┘    └───────────────────┘
```
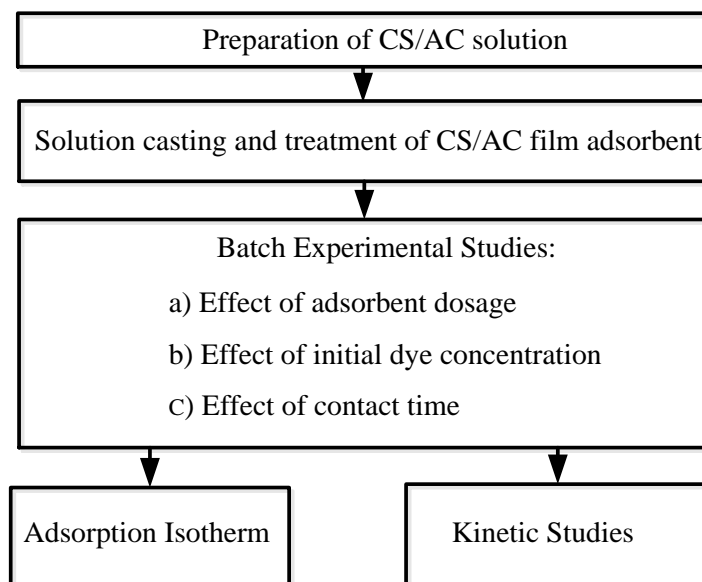
Figure 3.1: Diagram of Experimental Procedures

3.2 Materials and equipment

3.2.1 Materials

The CS has a 85 % deacetylated was purchased from Alfa Aesar. The AC was produced from coconut shell with size of 2 mm was then sieved until the particle size was less than 5µm. The average pore diameter is 5.27 nm. For the adsorption study, the BB dyes purchased from Sigma-Aldrich (M) Sdn. with a molecular weight of 867.68 g/mol were utilized as received. The CS powder was dissolved using acetic acid (AA) with a purity of 99.6 %. As a treatment for CS films, sodium hydroxide (NaOH) with a purity of 99 % is combined with 95 % denatured ethanol (EtOH). AA and NaOH were supplied by the Sigma-Aldrich (M) Sdn. Bhd, and EtOH by the Fisher Scientific (M) Sdn. Bhd. Deionized water was used throughout the experiment. Tables 3.1 shows the list of chemicals and Table 3.2 are the specification of BB dye.

Table 3.1: List of chemicals
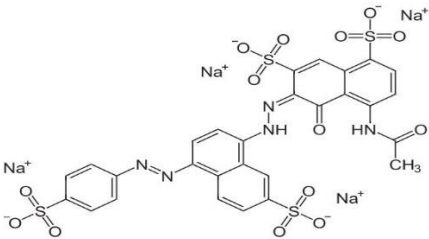
Chemical	Description	Supplier
Acetic acid	Molecular weight: 60 g/mol	
	Chemical formula: CH_3COOH	
	Density: 1.05 g/mL	Sigma-Aldrich
	Cas number: 64-19-7	
Activated carbon	Source: Coconut shells	
	Mesopore surface area: 502.31 m^2/g	
	Average pore diameter: 5.72 nm	-
	BET surface area: 658.44 m^2/g	

Table 3.1: Continued

Chitosan	Molecular weight: 1526.5 g/mol	
	Chemical Formula: $C_{56}H_{103}N_9O_{39}$	Alfa Aesar
	Cas number: 9012-76-4	
Deionized water	Chemical formula: H_2O	
	Density: 1 g/mL	Chemistry Lab
Ethanol	Molecular weight: 46.07 g/mol	
	Chemical formula: C_2H_5OH	
	Density: 0.798 g/mL	Fisher Scientific
	Cas number: 64-17-5	
Sodium hydroxide	Molecular weight:	
	Chemical formula:	
	Density: 2.13 g/mL	Sigma-Aldrich
	Cas number: 1310-73-2	

Table 3.2: The specification of BB (ALGAS ORGANICS InterLab et al., 2012)

Properties	Description	Supplier
Common name	Brilliant Black BN (BB)	Sigma-Aldrich
IUPAC name	Tetrasodium (6Z)-4-acetamido-5 oxo-6-[[7-sulfonato-4-(4-sulfonatophenyl)azo-1-naphthyl]hydrazono]naphthalene-1,7-disulfonate	
Molecular formula	$C_{28}H_{17}N_5Na_4O_{14}S_4$	
Cas number	2519-30-4	
Maximum wavelength	573 nm	
Chemical arrangement structure		

3.2.2 Equipment

In this study, some equipment was used in preparation of adsorbent and data collection for the adsorption experiment. Table 3.3 contains a list of the equipment utilized for this study.

Table 3.3: Equipment list utilized in this study

Equipment	Model	Purpose
Magnetic stirrers	IKA® C-MAG HS 7	To stir CS solution
Electronic balance	Shimadzu AY220	To measure the weight of AC, CS powder and NaOH pellet
Tip sonicator	Hielscher UP200S Ultrasonic	To disperse AC into CS solution
Bath sonicator	BRANSON 3800 Ultrasonic	To disperse AC into CS solution
UV-Visible spectrophotometer	Agilent Cary 60 UV-Vis	To measure absorbance of dye solution

3.3 Synthesis of puce CS and CS/AC composite films

3.3.1 Preparation of pure CS and CS/AC composite solutions.

The pure CS films and CS/AC composite films were prepared by using the solution casting method. Firstly, 10 wt.% of AA solution is prepared by dissolving 15 g of AA into 135 g of deionized water (DI) and stirred continuously by a magnetic stirrer. Then, 3.062 g of CS powder is added slowing dropwise into the AA solution to prepare a 2 wt. % of CS solution. The CS solution contain in the stirrer beaker was covered with aluminum foil was stirred continuously overnight at room temperature with speed of 625 rpm as shown in Figure 3.2 to allow to the solution to settle down. Next, 1.547 g of AC with 5µm size is dispersed into the CS solution for 1 wt. %. To ensure uniform dispersion, the AC is distributed into the CS solution using the bath ultrasonication for 30 minutes, as depicted in Figure 3.3, and then the tip ultrasonication with settings of 0.5 cycle and 60 % amplitude for 30 minutes, as depicted in Figure 3.4.
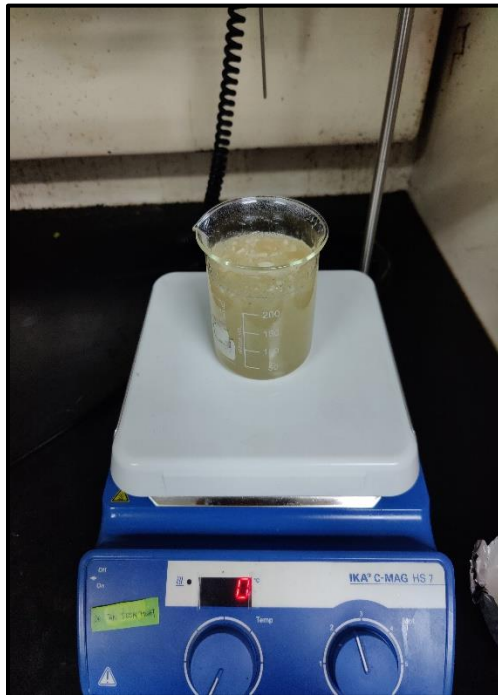
Figure 3.2: Stirring CS solution by magnetic stirrer at 625 rpm

Figure 3.3: 30 min of dispersion of AC into CS solution using a bath ultrasonicator.

Figure 3.4: 30 min of dispersion of AC into CS solution using a tip ultrasonicator.

3.3.2   Casting of CS and CS/AC composite films adsorbent

Casting of CS and CS/AC composite solution is done onto a petri dish whereby the solution is first measured to 30 ml using a beaker before it is poured onto the petri dish as shown Figure 3.5. The solution is left to dry inside the fume hood for 48 hours at room temperature. Then, a mixture solution consists of 3 wt. % of NaOH, 47 wt.% of EtOH and 50 wt. % of DI is prepared for the treatment of the CS and CS/AC films. The purpose of the treatment process is neutralized the AA contain in the adsorbent. The prepared treatment solution is poured into the dried films until it fully covered. Then the films are left inside the fume hood for 24 hours. Next the films are then washed thoroughly with DI to remove excess NaOH before being peeled off from the petri dish and dried at room temperature. The films are dried between A4 paper as shown in Figure 3.6.

a)

b)
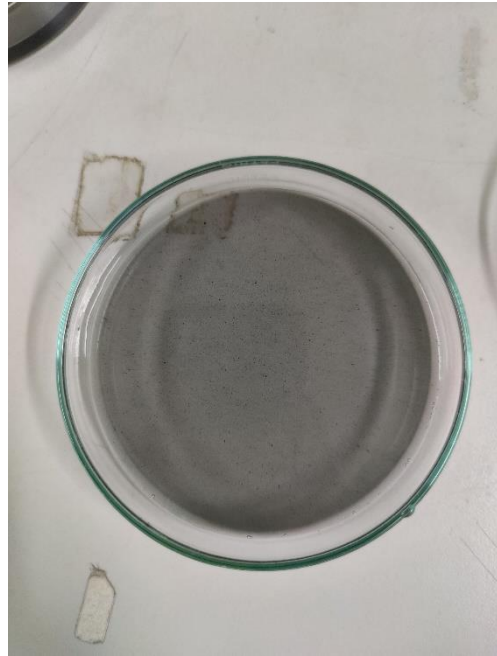
Figure 3.5: (a) CS and (b) CS/AC composite casting process

a)
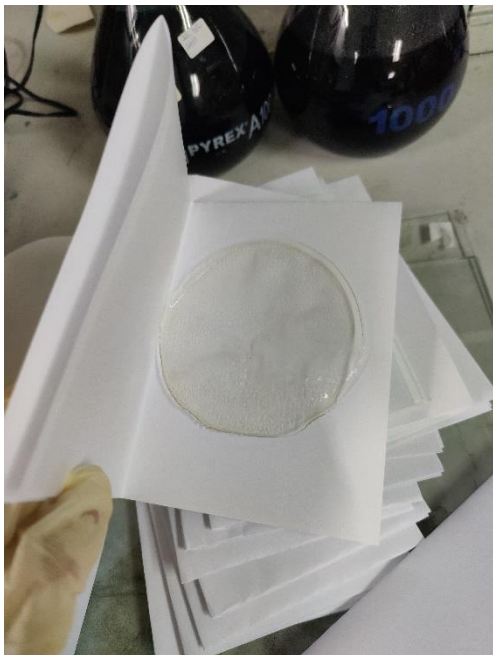
b)
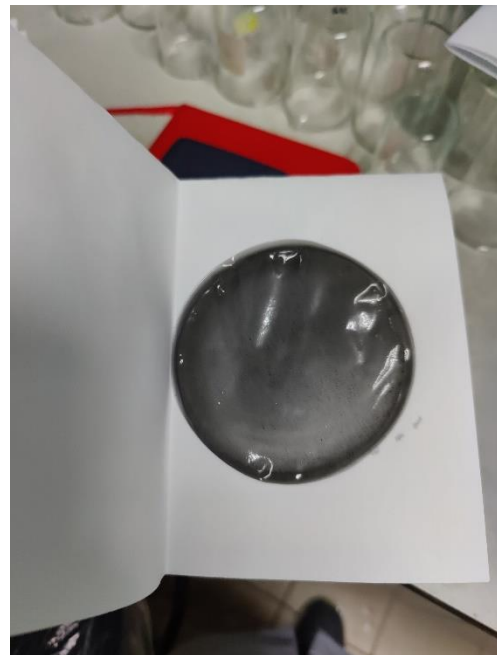
Figure 3.6: Drying process for (a) pure CS and (b) CS/AC between A4 paper

After both CS and CS/AC adsorbent films have been dried, each of the films is cut into a square shape with approximately 0.5 cm for each side. The square shape adsorbent films are weighted using the electronic balance as shown in Figure 3.7.

a)   b)
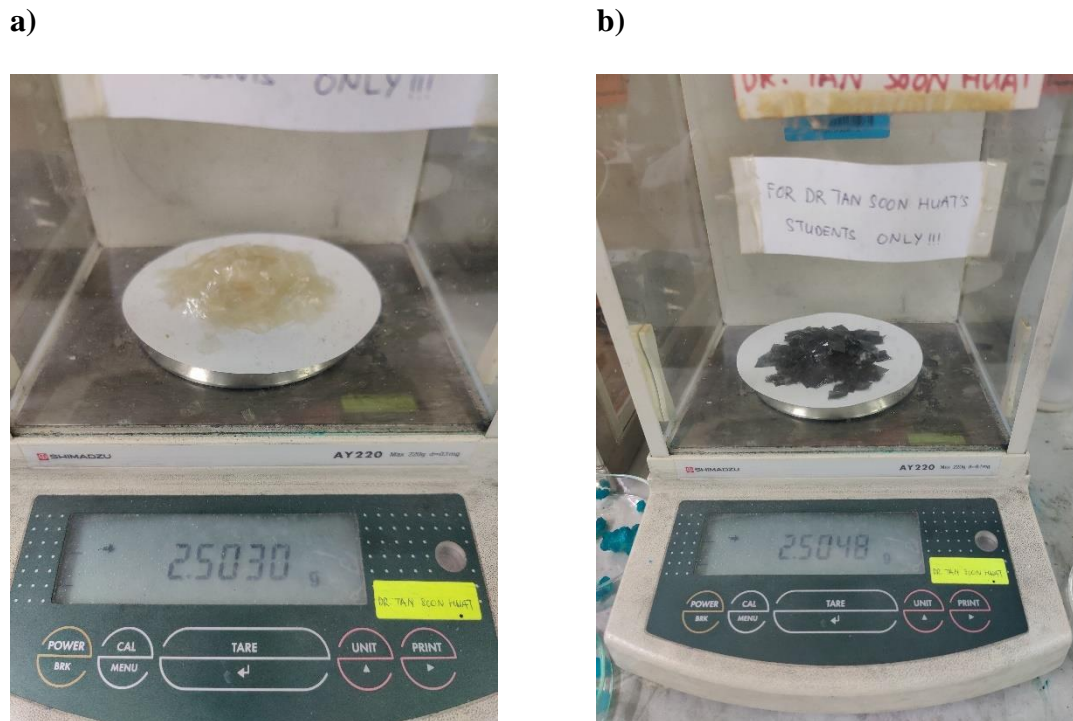
Figure 3.7: Weighing for (a) pure CS and (b) CS/AC using the electronic balance

3.4   Batch mode experiment on adsorption

Adsorption experiments are carried out in batch mode to determine the adsorption isotherm and its kinetics. This aids in understanding the effect adsorbent dosage, initial dye concentration and contact time on BB dye adsorption.

3.4.1 Preparation of adsorbate

Stock solution with concentration of 1000 mg/L which is equivalent to 1000 ppm is prepared by mixing 1 g of BB dye powder into 1000 mL of DI using a volumetric flask. For batch studies five different concentrations is prepared which are 40 mg/L, 80 mg/L, 120 mg/L, 160 mg/L and 200 mg/L by dilution process of the stock solution.

3.4.2 Sample analysis

4 ml of adsorbate solution was collected using plastic pipette to determine the dye concentration by using UV-visible spectrometer (Agilent Cary 60 UV-Vis) as displayed in Figure 3.8. The wavelength is set to 570 nm for BB dyes. The controlled deionized water sample was utilized as the blank sample. Calibration curve is done to determine the unknown concentration of sample by comparing the unknown to a set of standard samples of known concentration. The dye absorbance against dye concentration was represented.

Figure 3.8: UV-visible Spectrophotometer (Agilent Cary 60 UV-Vis)

3.4.3 Effect of adsorbent dosage

The effect of adsorbent dosage on the adsorption of BB dye was studied with 0.5 g, 1.0 g, 1.5 g, 2.0 g and 2.5 g of the mass of CS films. Different amount of CS films is added in a beaker filled with 150 mL BB dye with concentration of 120 mg/L. The experiment was conducted at room temperature without agitation to find the optimum adsorbent dosage for the adsorption of BB dye. The concentration of BB dye was determined at different time interval by using UV-Visible spectrophotometer until a steady state was obtained. The optimum adsorbent dosage found was used for CS/AC film to study the adsorption isotherms and kinetics.

3.4.4 Effect of initial dye concentration

Five different BB dye concentrations are prepared which are 40 mg/L, 80 mg/L, 120 mg/L, 160 mg/L and 200 mg/L in order to study the effect of initial dye concentration on the adsorption experiment. The different dye concentration is added into individual beaker with volume of 150 mL. Then, 2.5 g of CS films was immersed inside the dye solution and the concentration of BB dye was determined at different time interval by using UV-Visible spectrophotometer until a steady state was obtained. The experiment was conducted at room temperature without agitation to find the optimum initial dye concentration for the adsorption of BB dye onto the CS films. The optimum initial dye concentration found was used for CS/AC film to study the adsorption isotherms and kinetics.

3.4.5 Effect of Contact Time

To investigate the effect of contact time, different contact time intervals was taken for removal of BB dye. The 2.5 g of CS and CS/AC adsorbent were immersed into 150 mL of BB dye solution with a concentration of 40 mg/L. The UV-visible spectrophotometer was used to determine the concentration of BB solution at various time intervals until a steady state was achieved. The adsorption experiment was carried out at room temperature with no agitation.

3.4.6 Adsorption isotherms

The adsorption isotherm is studied by changing the contact time with the optimum adsorbent dosage and initial dye concentration. Three isotherms model which are Freundlich, Langmuir and Temkin isotherms is used. The applicability and suitability of the isotherm equation to the equilibrium data are compared by judging the values of the correlation coefficients, R^2 and normalized standard deviation, Δq_e. The removal efficiency (%t R) and the amount of adsorbate adsorbed per unit mass of adsorbent at equilibrium can be calculated using the Equations 3.1 and 3.2 shown below (qe).

$$\%R = \frac{C_0 - C_e}{C_0} \times 100\%$$

[Equation 3.1]

where:

C_e BB concentration at equilibrium (mg/L)

C_0 Initial BB concentration (mg/L)

$$q_e = \frac{(C_0 - C_e)V}{W}$$

[Equation 3.2]

where:

q_e Adsorption capacity at equilibrium (mg/g)

V   BB solution volume (L)

W   Mass of adsorbent (g)

CHAPTER FOUR

RESULTS AND DISCUSSIONS

4.1 Calibration Curve

Figure 4.1 depicts the calibration curve of dye absorbance against the concentrations of dye solution from 25 mg/L to 200 mg/L. The R^2 (correlation coefficient) value derived from the straight line on this graph was 0.9989. As the value was close to or equal to 1, it was deemed extremely accurate.

$$y = 0.018x + 0.0323$$
$$R^2 = 0.9989$$
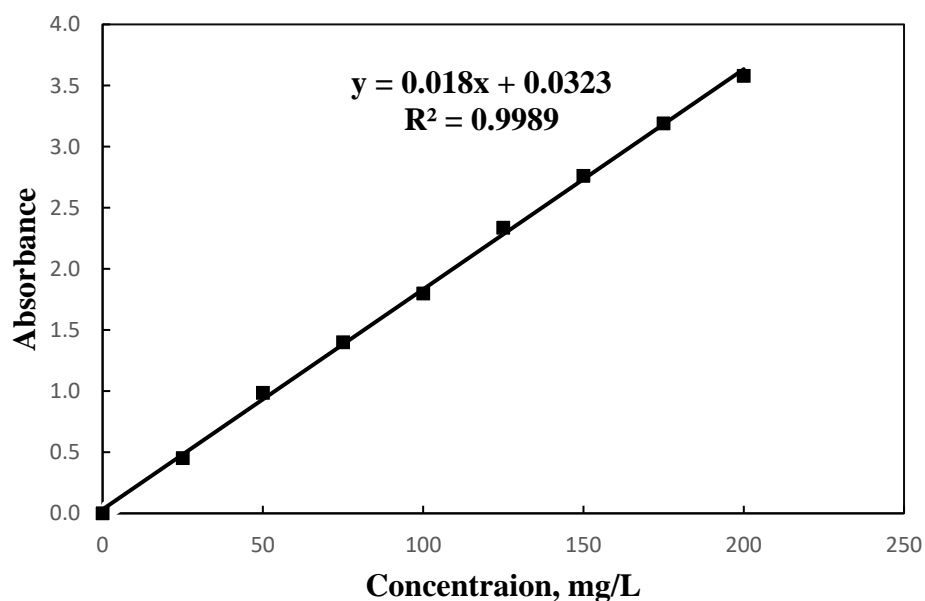
Figure 4.1: Calibration curve

4.2   Batch equilibrium studies

Batch equilibrium mode studies of BB removal by CS and CS/AC films for adsorbent dosage, initial dye concentration, and contact time were conducted in this section.

4.2.1   Effect of adsorbent dosage

The adsorption experiment was carried out at room temperature with different adsorbent dosage ranging from 0.5 g, 1.0 g, 1.5 g, 2.0 g and 2.5 g of CS films adsorbent at a constant BB dye initial concentration of 120 mg/L. The adsorption capacity against adsorption time and percentage removal of BB dye against adsorption time respectively for CS films adsorbent can be observed in Figure 4.2 and Figure 4.3 respectively. In Figure 4.2, it can be observed that the rate of adsorption is high at initially 300 min of the experiment for each adsorbent dosage. The adsorption rate become slower when it reaches a constant value whereby the adsorbent become saturated with dye and cannot adsorbed the dye further because it has reach equilibrium (Banerjee and Chattopadhyaya, 2017). Based on Figure 4.2, 0.5 g adsorbent dosage have a higher value for adsorption capacity, qe (23 mg/g) compared to adsorbent dosage of 2.5 g (7 mg/g). This is because the 0.5 g adsorbent dosage contain less availability vacant site and poor driving force as the time increases for the adsorption to occur compared to the 2.5 g adsorbent dosage. The 0.5 g adsorbent dosage become saturated faster with BB dye that have been attached to the vacant site of the CS films causing the highest value of qe at the final adsorption time compared to the other adsorbent dosage. This phenomenon is vice versa with the 2.5 g adsorbent dosage because it has more availability of vacant site and stronger driving force to adsorb the BB dye. Thus, the value of qe for the 2.5 g adsorbent is the lowest. Adsorption capacity seems is inversely proportional to the

36

adsorbent dosage since there are some of the adsorption sites remain unsaturated during the

adsorption process for higher adsorbent dosage.
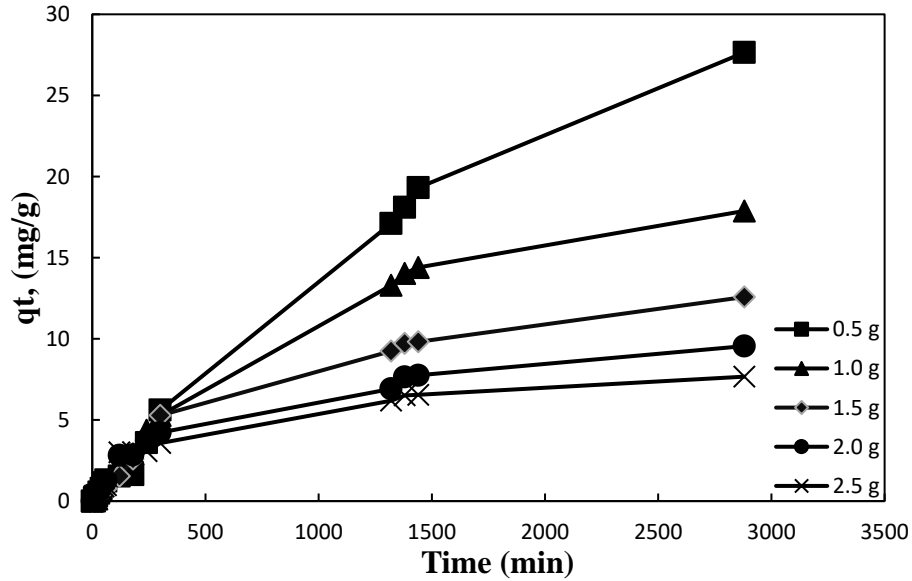
Figure 4.2: Adsorption capacity of CS films adsorbent against adsorption time at different
adsorbent dosage
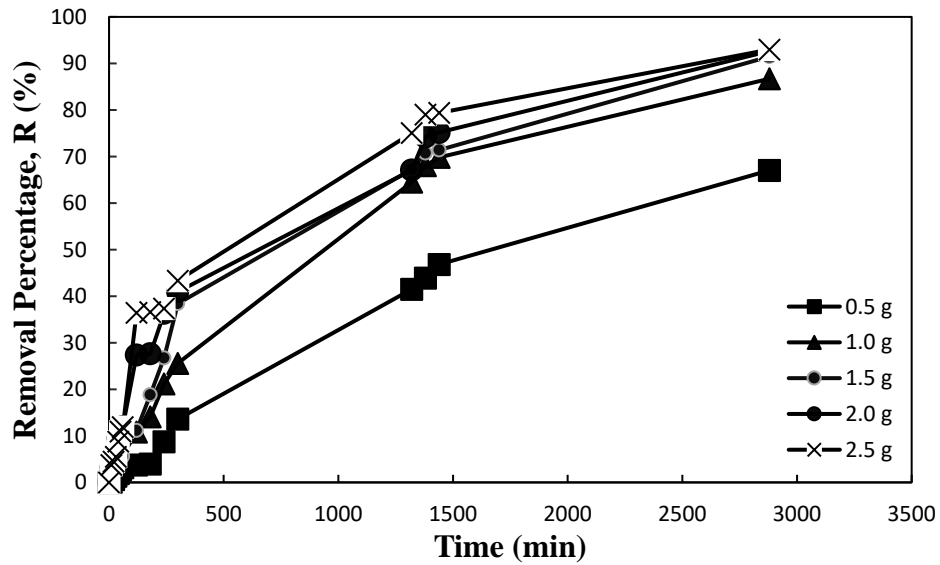
Figure 4.3: Removal percentage of BB dye against adsorption time at different adsorbent
dosage of CS films

Based on Figure 4.3, it can be observed that percentage removal of BB dye of the 2.5 g adsorbent dosage is the highest (93%) compared to the other adsorbent dosage. This is due to larger surface area provided by the 2.5 g adsorbent dosage for the removal of BB dye. The specific surface area of the adsorbent increased as the adsorbent dosage was increased. This increased the number of adsorption sites available to adsorb BB dye, resulting in a higher BB removal percentage. From the phenomena described above, it is found that as the amount of adsorbent film in solution increases, the percentage of BB dye removed increases gradually, but the value of qe decreases gradually. Therefore, 2.5 g adsorbent dosage is selected as the optimum value to conduct the next experiment which is the initial dye concentration and comparison of CS and CS/AC adsorbent performance.

4.2.2   Effect initial dye concentration and contact time

In this experiment, the adsorption was studied by manipulating the initial dye concentration with five different concentrations, which are 40 mg/L, 80 mg/L, 120 mg/L, 160 mg/L, and 200 mg/L, with a constant adsorbent dosage of 2.5 g which is the optimum adsorbent dosage for the CS films. Figure 4.4 shows the BB adsorption uptakes, qt against contact time at different initial dye concentrations while Figure 4.5 shows the removal percentage of BB dye by CS adsorbent films against contact time at different initial dye concentrations. Based on Figure 4.4, it can observe at beginning of the experiment, the adsorption uptakes increase rapidly for each initial dye concentration. This is due to the same phenomenon occur during the adsorbent dosage experiment whereby a lot of vacant site availability and driving force for adsorption process to takes place. As times pass by, the adsorption become slow and reach plateau due to the saturation of the vacant site by the BB

dye. 40 mg/L initial dye concentration shows the lowest value of adsorption uptakes which is 3 mg/g because there still many vacant site availabilities at the surface of the adsorbent. Furthermore, it was discovered that increasing the dye concentration increased the BB adsorption uptakes. The initial dye concentration served as a driving force to overcome the dye mass transfer resistance between the solid and aqueous phases. As the initial dye concentration increased, the driving force of the concentration gradient also increases, causing the BB adsorption uptakes to increase (Ebrahimian Pirbazari et al., 2014).

In Figure 4.5, it can be noticed that the adsorption for 40 mg/L initial dye concentration has the highest rate of dye removal at the beginning of 500 min of the experiment. The concentration of 40 mg/L BB dye solution reaches a plateau graph earlier compared to the other concentrations. This shows that no more or less dye left that can adsorb by the adsorbent films. This is because, the amount of adsorbate contain in the dye solution is the lowest compared to the other initial dye concentrations. As the contact time increases, the rate of removal of BB dye become slower due to adsorbent vacant site become saturated. It can be observed that all of the initial dye concentration achieves 80 % and above for percentage removal of BB dye. The highest percentage of BB dye removal is 96 % that was achieved by the 40 mg/L initial dye concentration. Therefore, 40 mg/L initial dye concentration is selected as the optimum parameter to be studied for the CS/AC adsorbent films. Figure 4.6 shows the photographs of the BB solution before and after the adsorption by the CS adsorbent films. The solution is insert into the cuvette to have a clearer image difference before and after the experiment. Figure 4.6 (a)(b)(1) shows a cuvette contain DI as blank sample. Figure 4.6 (a)(b)(2) shows a cuvette containing 40 mg/L BB dye

concentration while (3) to (6) shows 80 mg/L, 120 mg/L, 160 mg/L and 200 mg/L of BB dye concentration respectively.
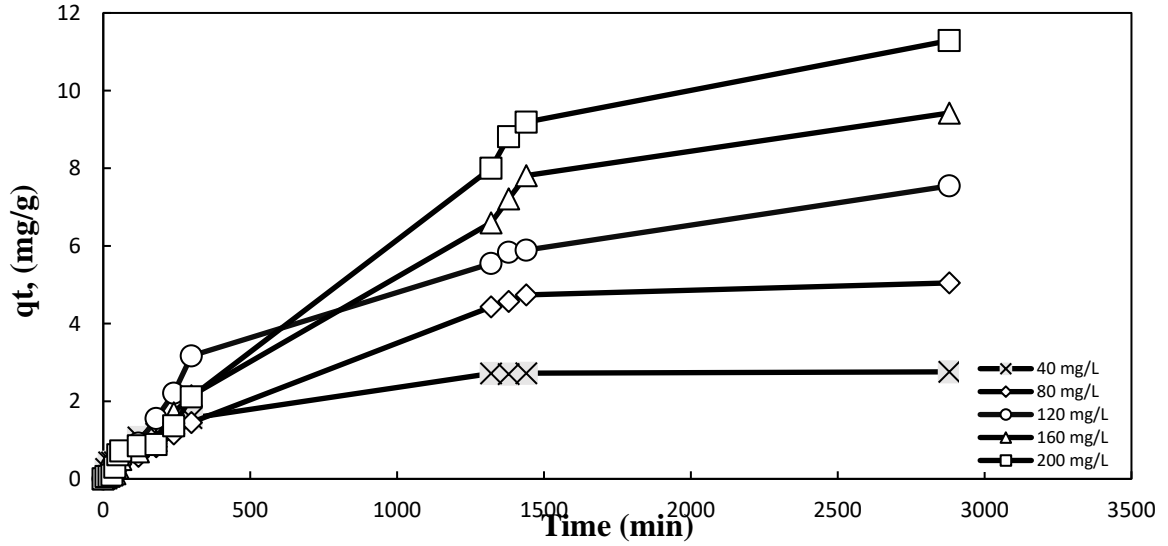
Figure 4.4: BB adsorption uptake against contact time at different initial dye concentrations
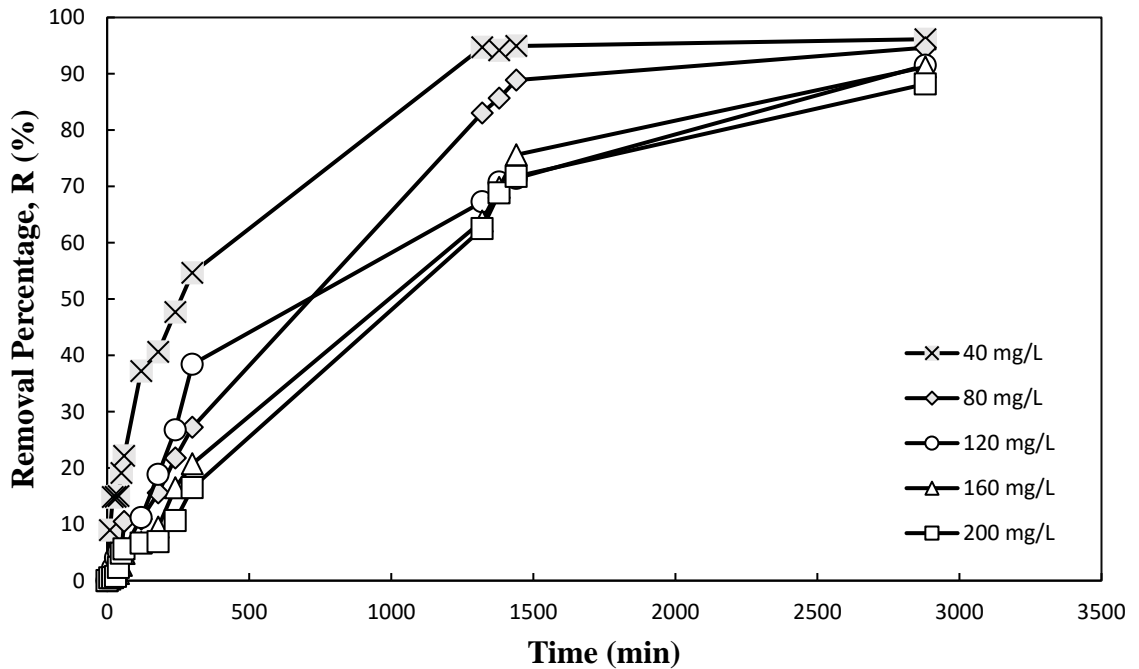
Figure 4.5: Removal percentage of BB dye by CS films adsorbent against contact time at different initial dye concentrations
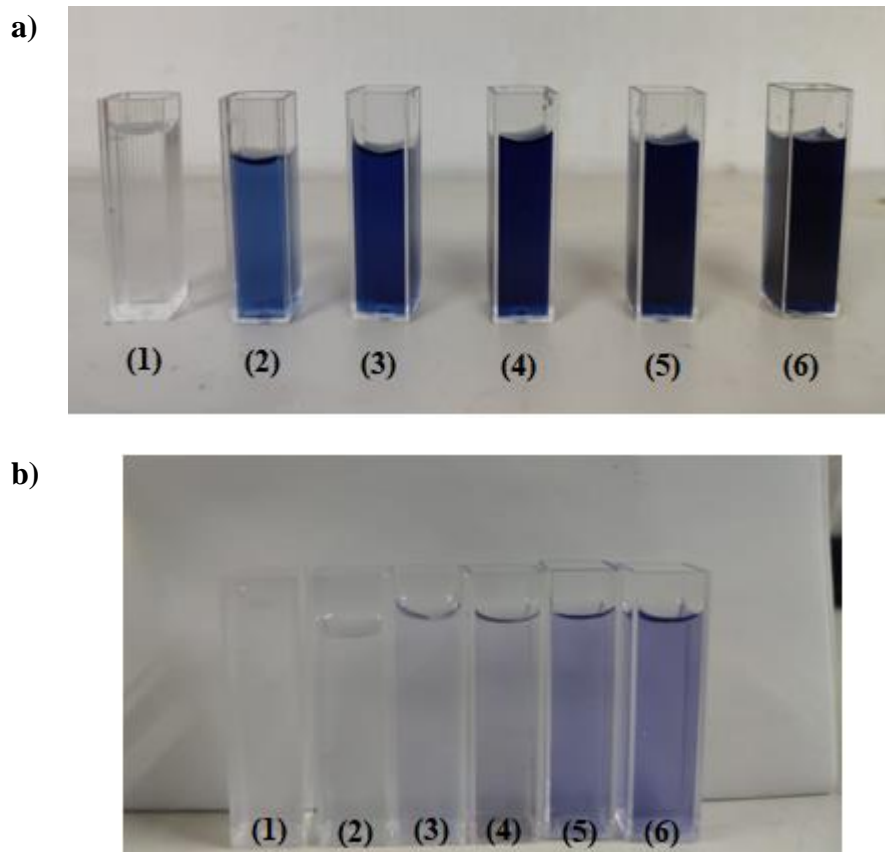
Figure 4.6: Before (a) and after (b) adsorption by the CS adsorbent films, images of the BB solution are captured.

4.2.3 Comparison of CS and CS/AC adsorbent films

In this part of experiment, the adsorption of BB dye is studied by using 2.5 g of CS/AC adsorbent films with initial dye concentration of 40 mg/L. The adsorption capacity and the removal percentage of BB dye by the CS/AC adsorbent films is compared with the pure CS adsorbent films. Figure 4.7 shows the adsorption capacity against adsorption time for CS and CS/AC adsorbent films. Based on Figure 4.7, it can be noticed that the rate of adsorption for both type of adsorbent increase rapidly at the early stage of the experiment. Both CS and CS/AC adsorbent films have a similar graph profile at the beginning of

adsorption time towards the end. The pure CS adsorbent film has a higher value of adsorption capacity which is 2.8 mg/g compared to CS/AC adsorbent film which is at 2.6 mg/g. This shows that the CS films has reach equilibrium faster as opposed to the CS/AC films. This is because CS films has a smaller surface area in contrast with CS/AC films due to addition of AC in the adsorbent. AC has an adsorption pores regions within the particle that adsorb more dye while the pure CS films only depends on the surface of the adsorbent (Baby et al., 2019). AC have a highly porous structure that consists of three region which are macro, meso and micro pores as shown in Figure 4.8. This pore assists the adsorbent in increasing the surface area. Therefore CS/AC films have a higher availability of vacant site to attach the BB dye comparing with the pure CS films.

Figure 4.9 shows the removal percentage of BB dye by CS films adsorbent against adsorption time for CS and CS/AC adsorbent films. In Figure 4.9, it can be observed that the CS films have better removal percentage of BB dye at the first 500 min of the adsorption experiment. This is because, the adsorption process can occur smoothly without any disturbance compared to the CS/AC film which contain AC particle embedded inside the CS polymer. The AC particle can act as a disturbance to the adsorption process due to imbalance charge produce between the CS and AC surface (Bernal et al., 2018). This can cause a small repulsion force on the surface of the adsorbent causing difficult for the dye to attach to the vacant site. When the adsorption time increases, both CS and CS/AC films have almost the same value removal percentage of BB dye. The removal percentage of BB dye by the CS films is 96% while the CS/AC films is 97%. This shows that adding the AC into the CS polymer does not show a significant difference in terms of the performance of the adsorbent.
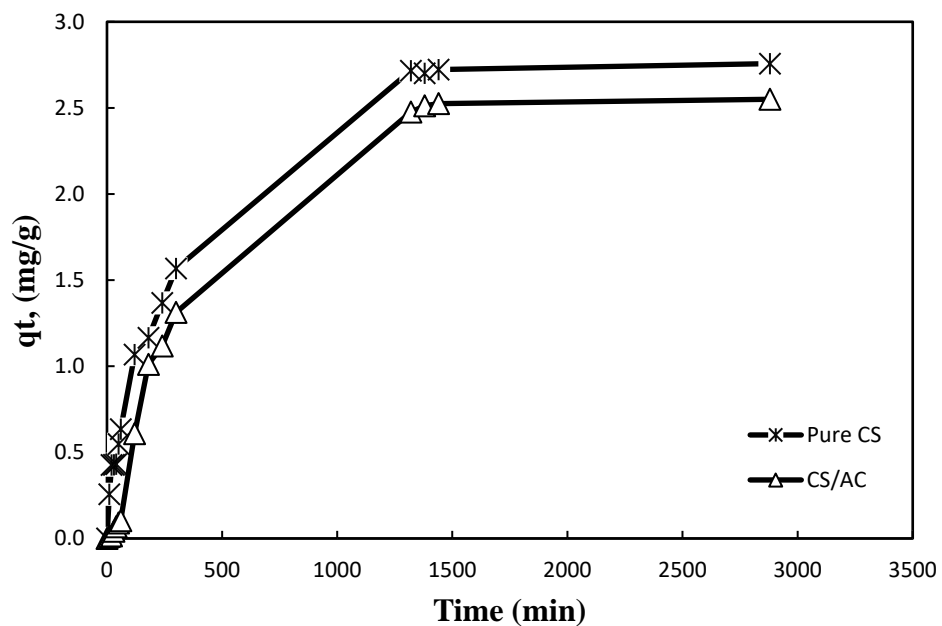
Figure 4.7: Adsorption capacity against adsorption time for CS and CS/AC adsorbent films
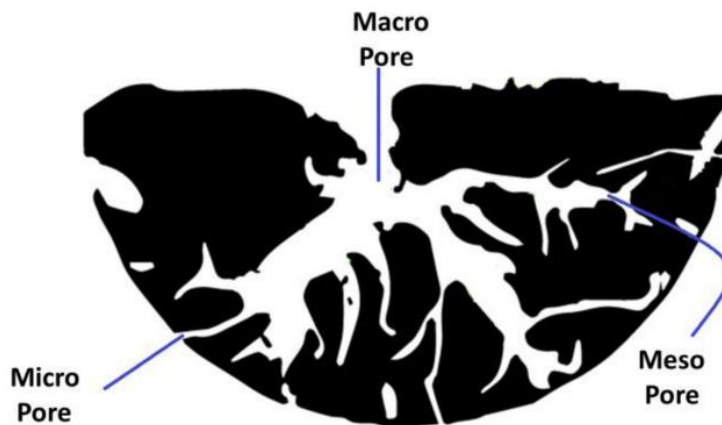
Figure 4. 8: Different types of pores in AC (Baby et al., 2019)
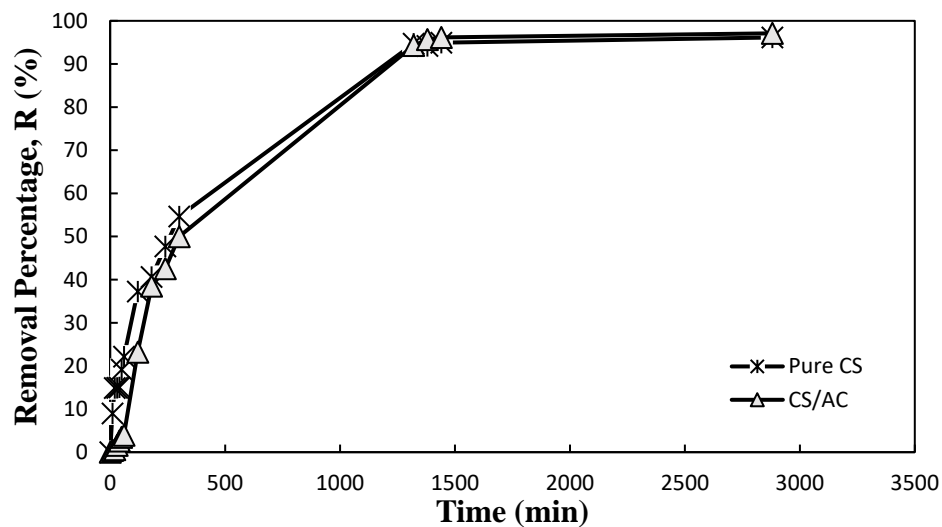
Figure 4.9: Removal percentage of BB dye by CS films adsorbent against adsorption time for CS and CS/AC adsorbent films

Figure 4.10 shows the photographs of the BB solution before and after the adsorption by the CS/AC adsorbent films. Figure 4.10 (a) shows the BB dye solution with concentration of 40 mg/L before the adsorption experiment while Figure 4.10 (b) show the BB solution after the adsorption experiment with the adsorbent being removed.
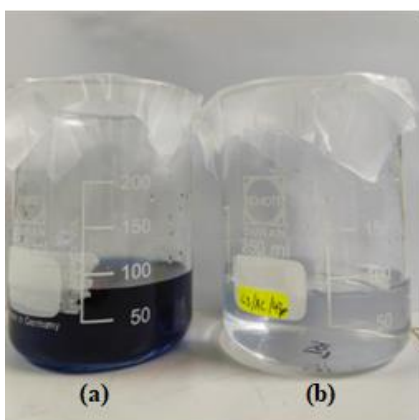
Figure 4.10: Before (a) and after (b) adsorption by the CS/AC adsorbent films, images of the BB solution are captured.

4.3 Adsorption isotherms

Understanding and interpreting adsorption isotherms is essential for enhancing adsorption mechanism pathways and designing an effective solid-liquid adsorption system (El-Khaiary, 2008). The adsorption isotherm can reveal the distribution of dye molecules between the solid and liquid phases once equilibrium is reached. Using Langmuir, Freundlich, and Temkin isotherms, the adsorption equilibrium data obtained from the BB removal by CS and CS/AC can be analyzed in this study. In this study, adsorption isotherms are determined based on the optimal batch experiment parameters of 2.5 g adsorbent dosage and 40 mg/L initial BB dye concentration. Using Equation 4.1, 4.2, and 4.3, a linear graph variant of the Langmuir, Freundlich, and Temkin isotherms model were utilized to fit the equilibrium data. The symbols used in Equations 4.1, 4.2, and 4.3 are defined in Chapter 2.

$$\frac{1}{q_e} = \frac{1}{q_m} + \frac{1}{q_m K_L C_e} \qquad \text{[Equation 4.1]}$$

$$\log q_e = \log K_F + \left(\frac{1}{n_F}\right) \log C_e \qquad \text{[Equation 4.2]}$$

$$q_e = B \ln a_t + B \ln C_e \qquad \text{[Equation 4.3]}$$

Figures 4.11, 4.12, and 4.13 illustrate the linear graph isotherm plots based on experimental data and the correlations by the three models for CS and CS/AC, respectively. The constant isotherm values were calculated from the slope and intercept of straight-line plots, and their correlation coefficients, R^2, are reported in Table 4.1. The value of R_L, the dimensionless separation factor, is derived using Equation 4.4.

$$R_L = \frac{1}{(1 + K_L C_0)}$$
<div align="right">[Equation 4.4]</div>
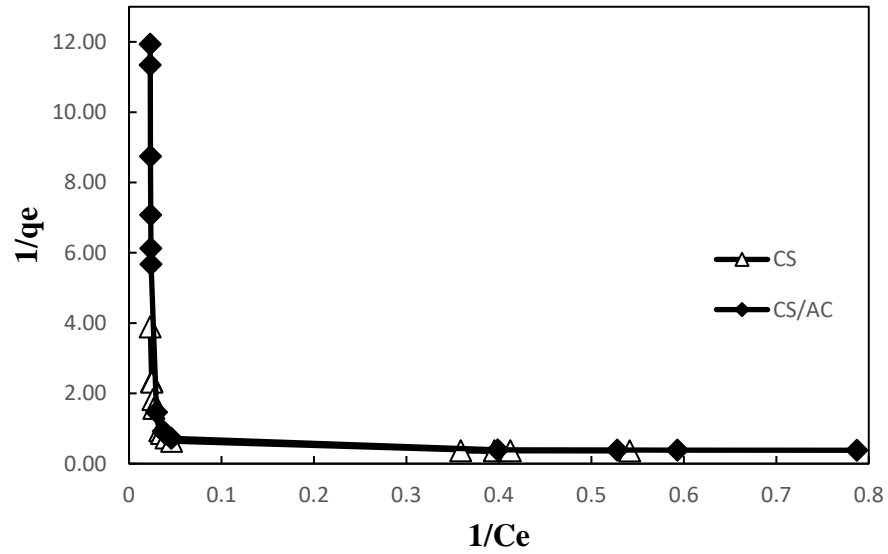
Figure 4.11: Langmuir isotherms for BB adsorption on CS and CS/AC adsorbent films
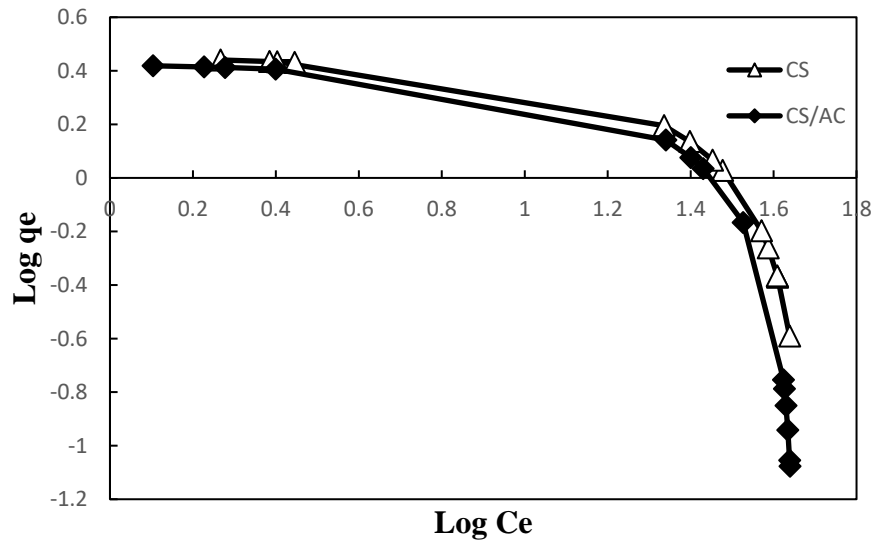
Figure 4.12: Freundlich isotherms for BB adsorption on CS and CS/AC adsorbent films
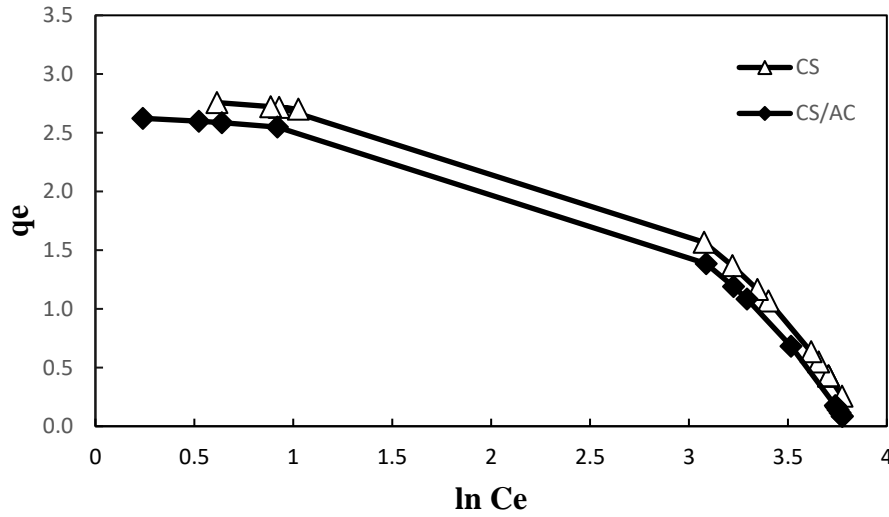
Figure 4.13: Temkin isotherms for BB adsorption on CS and CS/AC adsorbent films

Table 4.1: Adsorption isotherms' parameters and correlation coefficients for BB adsorption by CS and CS/AC adsorbent films

Isotherm	Parameters	Adsorbents	
		CS	CS/AC
Langmuir	q_m (mg/g)	0.5973	0.0475
	K_L (L/mg)	-0.5506	-0.5985
	R^2	0.2701	0.1129
Freundlich	K_F (mg/g(L/mg)$^{1/n}$)	4.6665	6.2834
	n_F	-1.8426	-0.9617
	R^2	0.7242	0.5295
Temkin	B (J/mol)	-0.7791	-0.7469
	a_t (L/g)	0.0117	0.0165
	R^2	0.9313	0.9065

Based on Table 4.1 it can be concluded that the only model that fit the experimental data is the Temkin isotherms because of the R^2 value for both CS and CS/AC films is above 0.9 which is near to unity. The R^2 for the CS films is 0.9313 while the CS/AC films is 0.9065. The Temkin isotherm model assumes that the adsorption energy of all molecules decreases linearly with increasing adsorbent surface coverage and that adsorption is characterized by a uniform distribution of binding energies, up to a maximum binding energy (Piccin et al., 2011). The value B is -0.7791 J/mol and -0.7469 J/mol for CS and CS/AC films respectively, indicates the adsorption process is endothermic reaction (Sharma et al., 2016).

The other two model which are Langmuir and Freundlich model does not suitable for the experimental data because the correlation coefficient does not achieve 0.9. Furthermore, the value of separation factor, R_L gave a negative value since the Langmuir adsorption constant, K_L are also negative for both type of adsorbent. Thus, the Langmuir model is rejected in this study. For the Freundlich isotherm, the value of Freundlich constant, n_F shows a negative value for both type adsorbent indicates the n_F is less than 1 showing the experimental data is unfavorable for this model.

4.4   Adsorption kinetic studies

To determine the kinetics of BB adsorption by CS and CS/AC adsorbent films, experimental data were fit into two models: PFO and PSO. The equation and adsorption parameters of these kinetic models were discussed in Chapter 2. The adsorption kinetic study was conducted at the optimum parameter of 2.5 g adsorbent dosage and 40 mg/L initial BB dye concentration. Figures 4.14 and 4.15 represented the linearized plots of the PFO and PSO kinetic models for CS and CS/AC adsorbent films, respectively.
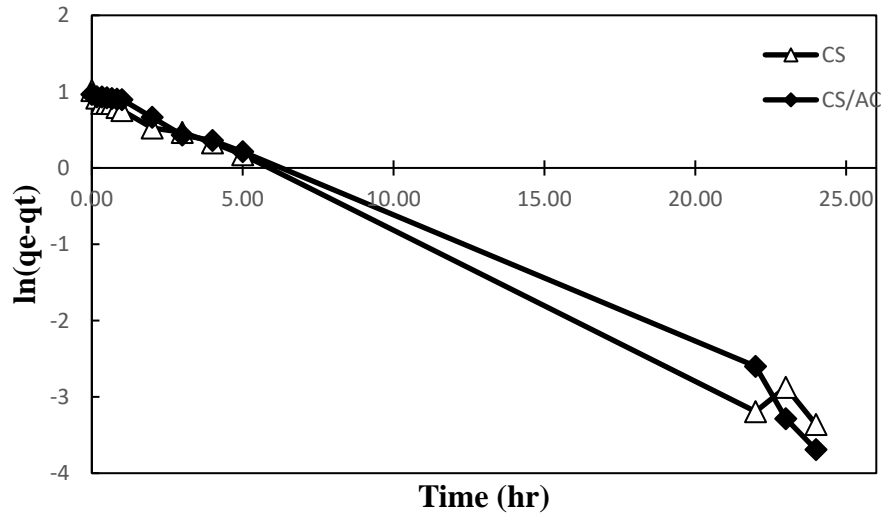
Figure 4.14: Plots of linearized PFO kinetic models for CS and CS/AC adsorbent films
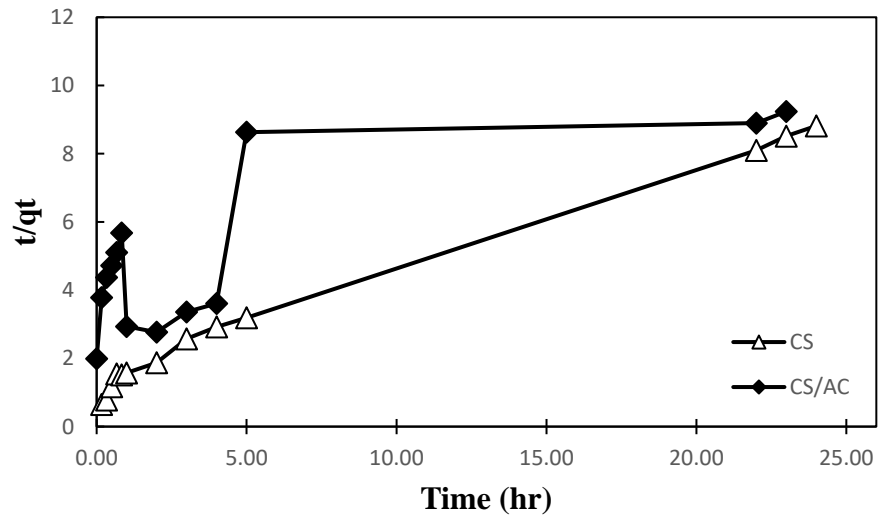
Figure 4.15: Plots of linearized PSO kinetic models for CS and CS/AC adsorbent films

Table 4.2: Kinetic value of BB dye adsorption on CS and CS/AC adsorbent films.

Adsorbent	Experimental data	PFO parameters			PSO parameters		
	qe (mg/g)	k_1 (hr^{-1})	qe cal (mg/g)	R^2	k_2 (g/mg.hr)	qe cal (mg/g)	R^2
CS	2.7570	0.1836	2.8019	0.9955	0.0851	3.1289	0.9887
CS/AC	2.6228	0.1779	2.6161	0.9919	0.0439	4.3554	0.7868

The kinetic value of BB dye adsorption on CS/AC adsorbent films are summarized in Table 4.2. On the basis of the close to unity R^2 value, it can be observed that the experimental data obtained from both types of film adsorbents fit better in the PFO kinetic model than in the PSO kinetic model. R^2 for the CS films adsorbent was 0.9955, while R^2 for the CS/AC films adsorbent was 0.9919. It was discovered that both CS and CS/AC adsorbent films followed the PFO kinetic model. In addition, the PFO qe values for both adsorbents were considerably closer to the experimental qe values than the PSO qe values. Physisorption could be the rate-limiting step in adsorption processes if the PFO kinetic model is the best fit for this study.

CHAPTER FIVE

CONCLUSION AND RECOMMENDATIONS

5.1   Conclusion

In this study, the synthesis of CS and CS/AC composite adsorbent in the form of films is recommended to remove the BB dye from the aqueous solution because it is easier to be recovered and replace with the fresh absorbents. Both CS and CS/AC composite adsorbent films were effective for BB dye removal from the aqueous solution. In terms of the effect of adsorbent dosage, there was a decrease in BB adsorption capacity with respect to increasing of adsorbent dosage from 27.64 mg/g to 7.67 mg/g for CS adsorbent films and it is found that the 2.5 g adsorbent dosage is the optimum parameter for the CS adsorbent films. In the matter of the effect of initial dye concentration and contact time, the amount of BB dye adsorbed onto the CS adsorbent films increases with respect to time and remained constant at the end of the experiment that give an adsorption capacity ranging from 2.76 mg/g to 11.29 mg/g. It found that the optimum initial dye concentration for this experiment was the 40 mg/L. It was found that in terms of the dye removal percentage, both CS and CS/AC provided almost similar results which were 96% and 97%, respectively. Thus, AC might not be the suitable filler for CS film for BB dye removal.

Adsorption isotherm shows that both CS and CS/AC composite adsorbent films were best described in Temkin isotherms model which indicates the adsorption heat of all molecules decreases linearly with the increase in coverage of the adsorbent surface of CS and CS/AC adsorbent films. Meanwhile, kinetic studies revealed that the PFO kinetic model

fit both adsorbents better than the PSO kinetic model, as measured by the R^2, which was close to unity.

5.2 Recommendations

The following were some of the recommendations for future work:

1. To study the performance of CS and CS/AC adsorbent films using the real industrial wastewater sample.
2. To investigate the mechanical strength of CS and CS/AC films
3. To study the regeneration and reusability of adsorbent in reducing waste and maintain the environmental sustainability.

REFERENCE

Achparaki, M., Thessalonikeos, E., Tsoukali, H., Mastrogianni, O., Zaggelidou, E., Chatzinikolaou, F., Vasilliades, N., Raikos, N., Isabirye, M., Raju, D.V.., Kitutu, M., Yemeline, V., Deckers, J., J. Poesen Additional, 2012. We are IntechOpen , the world ' s leading publisher of Open Access books Built by scientists , for scientists TOP 1 %. Intech 13.

Adegoke, K.A., Bello, O.S., 2015. Dye sequestration using agricultural wastes as adsorbents. Water Resour. Ind. 12, 8–24. https://doi.org/10.1016/j.wri.2015.09.002

Ahmad, M.A., Ahmad, N., Bello, O.S., 2015. Adsorption Kinetic Studies for the Removal of Synthetic Dye Using Durian Seed Activated Carbon. J. Dispers. Sci. Technol. 36, 670–684. https://doi.org/10.1080/01932691.2014.913983

Ai, L., Jiang, J., 2010. Fast Removal of Organic Dyes from Aqueous Solutions by AC/Ferrospinel Composite. Desalination 262, 134–140. https://doi.org/10.1016/j.desal.2010.05.059

ALGAS ORGANICS InterLab, Confidential, H., Aldrich, Usp, A., 2012. 产品规格书 Product Specification. Sigma-Aldrich 63103.

Aranaz, I., Mengibar, M., Harris, R., Panos, I., Miralles, B., Acosta, N., Galed, G., Heras, A., 2009. Functional Characterization of Chitin and Chitosan. Curr. Chem. Biol. https://doi.org/http://dx.doi.org/10.2174/2212796810903020203

Arun Prasad, A. S., Bhaskara Rao, K.V., 2010. Physico Chemical Characterization of

Textile Effluent and Screening for Dye Decolorizing Bacteria. Glob. J. Biotechnol. Biochem.

Baby, R., Saifullah, B., Hussein, M.Z., 2019. Carbon Nanomaterials for the Treatment of Heavy Metal-Contaminated Water and Environmental Remediation. Nanoscale Res. Lett. 14. https://doi.org/10.1186/s11671-019-3167-8

Bafana, A., Devi, S.S., Chakrabarti, T., 2011. Azo dyes: past, present and the future. Environ. Rev. 19, 350–371. https://doi.org/10.1139/a11-018

Banerjee, S., Chattopadhyaya, M.C., 2017. Adsorption characteristics for the removal of a toxic dye, tartrazine from aqueous solutions by a low cost agricultural by-product. Arab. J. Chem. 10, S1629–S1638. https://doi.org/10.1016/j.arabjc.2013.06.005

Bernal, V., Giraldo, L., Moreno-Piraján, J., 2018. Physicochemical Properties of Activated Carbon: Their Effect on the Adsorption of Pharmaceutical Compounds and Adsorbate–Adsorbent Interactions. C 4, 62. https://doi.org/10.3390/c4040062

Bhatt, M., Patel, M., Rawal, B., Novotný, Č., Molitoris, H.P., Šašek, V., 2000. Biological decolorization of the synthetic dye RBBR in contaminated soil. World J. Microbiol. Biotechnol. 16, 195–198. https://doi.org/10.1023/A:1008937503675

Carneiro, P.A., Nogueira, R.F.P., Zanoni, M.V.B., 2007. Homogeneous photodegradation of C.I. Reactive Blue 4 using a photo-Fenton process under artificial and solar irradiation. Dye. Pigment. 74, 127–132. https://doi.org/10.1016/j.dyepig.2006.01.022

Chang, Y.-C., Chen, D.-H., 2005. Adsorption kinetics and thermodynamics of acid dyes on a carboxymethylated chitosan-conjugated magnetic nano-adsorbent. Macromol. Biosci.

5, 254–261. https://doi.org/10.1002/mabi.200400153

Chen, L., Hao, H., Zhang, W., Shao, Z., 2020. Adsorption mechanism of copper ions in aqueous solution by chitosan–carboxymethyl starch composites. J. Appl. Polym. Sci. 137, 48636. https://doi.org/https://doi.org/10.1002/app.48636

Chowdhury, Z.K., 2013. Activated carbon : solutions for improving water quality.

Crini, G., 2006a. Non-conventional low-cost adsorbents for dye removal: A review. Bioresour. Technol. 97, 1061–1085. https://doi.org/10.1016/j.biortech.2005.05.001

Crini, G., 2006b. Non-conventional low-cost adsorbents for dye removal: A review. Bioresour. Technol. 97, 1061–1085. https://doi.org/https://doi.org/10.1016/j.biortech.2005.05.001

Cui, D., Guo, Y.-Q., Cheng, H.-Y., Liang, B., Kong, F.-Y., Lee, H.-S., Wang, A.-J., 2012. Azo dye removal in a membrane-free up-flow biocatalyzed electrolysis reactor coupled with an aerobic bio-contact oxidation reactor. J. Hazard. Mater. 239–240, 257–264. https://doi.org/10.1016/j.jhazmat.2012.08.072

Desta, M.B., 2013. Batch Sorption Experiments: Langmuir and Freundlich Isotherm Studies for the Adsorption of Textile Metal Ions onto Teff Straw (*Eragrostis tef*) Agricultural Waste. J. Thermodyn. 2013, 375830. https://doi.org/10.1155/2013/375830

Donnet, J.-B., 1995. 95/04670 Carbon black science and technology, Fuel and Energy Abstracts. https://doi.org/10.1016/0140-6701(95)96467-q

Ebrahimian Pirbazari, A., Saberikhah, E., Badrouh, M., Emami, M.S., 2014. Alkali treated Foumanat tea waste as an efficient adsorbent for methylene blue adsorption from

aqueous solution. Water Resour. Ind. 6, 64–80. https://doi.org/10.1016/j.wri.2014.07.003

El-Khaiary, M.I., 2008. Least-squares regression of adsorption equilibrium data: comparing the options. J. Hazard. Mater. 158, 73–87. https://doi.org/10.1016/j.jhazmat.2008.01.052

Fonseca, Jefferson C S da Silva A4., D B França A4., Francisco Rodrigues A4., Dyego M Oliveira A4.,Pollyana Trigueiro A4., E C Silva Filho A4., M G., 2021. What happens when chitosan meets bentonite under microwave-assisted conditions? Clay-based hybrid nanocomposites for dye adsorption. Colloids and surfaces v. 609, 125584--2021 v.609. https://doi.org/10.1016/j.colsurfa.2020.125584

Food and Agriculture Organization of the United Nations. The State of World Fisheries and Aquaculture (FAO, 2014). - Google Search [WWW Document], n.d. URL https://www.google.com/search?q=Food+and+Agriculture+Organization+of+the+United+Nations.+The+State+of+World+Fisheries+and+Aquaculture+(FAO%2C+2014).&oq=Food+and+Agriculture+Organization+of+the+United+Nations.+The+State+of+World+Fisheries+and+Aquaculture+(FAO%2C+2014).&aqs=chrome..69i57.1012j0j15&sourceid=chrome&ie=UTF-8 (accessed 6.21.22).

Freundlich, H., 1907. Über die Adsorption in Lösungen. Zeitschrift für Phys. Chemie 57U, 385–470. https://doi.org/doi:10.1515/zpch-1907-5723

Ganiyu, S.A., Ajumobi, O.O., Lateef, S.A., Sulaiman, K.O., Bakare, I.A., Qamaruddin, M., Alhooshani, K., 2017. Boron-doped activated carbon as efficient and selective adsorbent for ultra-deep desulfurization of 4,6-dimethyldibenzothiophene. Chem. Eng.

J. 321, 651–661. https://doi.org/https://doi.org/10.1016/j.cej.2017.03.132

Guo, J., Chen, S., Liu, L., Li, B., Yang, P., Zhang, L., Feng, Y., 2012. Adsorption of dye from wastewater using chitosan–CTAB modified bentonites. J. Colloid Interface Sci. 382, 61–66. https://doi.org/https://doi.org/10.1016/j.jcis.2012.05.044

Huo, M.X., Jin, Y.L., Sun, Z.F., Ren, F., Pei, L., Ren, P.G., 2021. Facile synthesis of chitosan-based acid-resistant composite films for efficient selective adsorption properties towards anionic dyes. Carbohydr. Polym. 254, 117473. https://doi.org/10.1016/j.carbpol.2020.117473

Husain, Q., 2006. Potential Applications of the Oxidoreductive Enzymes in the Decolorization and Detoxification of Textile and Other Synthetic Dyes from Polluted Water: A Review. Crit. Rev. Biotechnol. 26, 201–221. https://doi.org/10.1080/07388550600969936

IUPAC, 1979. International Union of Manual of Symbols and Terminology for Physicochemical Quantities. Pure Appl. Chem. 51, 1–41.

Jana, S., Saikia, A., Purkait, M.K., Mohanty, K., 2011. Chitosan based ceramic ultrafiltration membrane: Preparation, characterization and application to remove Hg(II) and As(III) using polymer enhanced ultrafiltration. Chem. Eng. J. 170, 209–219. https://doi.org/10.1016/j.cej.2011.03.056

Jin Li, J.C., 2013. Parametric Optimization of Extracellular Chitin Deacetylase Production by Scopulariopsis brevicaulis. J. Biocatal. Biotransformation 02, 4–8. https://doi.org/10.4172/2324-9099.1000103

John Kasongo, K., Tubadi, D.J., Bampole, L.D., Kaniki, T.A., Kanda, N.J.M., Lukumu, M.E., 2020. Extraction and characterization of chitin and chitosan from Termitomyces titanicus. SN Appl. Sci. 2. https://doi.org/10.1007/s42452-020-2186-5

J.S.Piccin, M.L.G.Vieira, J.O.Gonçalves, G.L.Dotto, L.A.A.Pinto, 2009. Adsorption of FD&C Red No. 40 by chitosan: Isotherms analysis. J. Food Eng. 95, 16–20. https://doi.org/10.1016/j.jfoodeng.2009.03.017

Kakavandi, B., Kalantary, R.R., Farzadkia, M., Mahvi, A.H., Esrafili, A., Azari, A., Yari, A.R., Javid, A.B., 2014. Enhanced chromium (VI) removal using activated carbon modified by zero valent iron and silver bimetallic nanoparticles. J. Environ. Heal. Sci. Eng. 12, 115. https://doi.org/10.1186/s40201-014-0115-5

Katheresan, V., Kansedo, J., Lau, S.Y., 2018. Efficiency of various recent wastewater dye removal methods: A review. J. Environ. Chem. Eng. 6, 4676–4697. https://doi.org/10.1016/j.jece.2018.06.060

Khajavian, M., Salehi, E., Vatanpour, V., 2020. Chitosan/polyvinyl alcohol thin membrane adsorbents modified with zeolitic imidazolate framework (ZIF-8) nanostructures: Batch adsorption and optimization. Sep. Purif. Technol. 241, 116759. https://doi.org/https://doi.org/10.1016/j.seppur.2020.116759

Khan, N.A., Bhadra, B.N., Jhung, S.H., 2018. Heteropoly acid-loaded ionic liquid@metal-organic frameworks: Effective and reusable adsorbents for the desulfurization of a liquid model fuel. Chem. Eng. J. 334, 2215–2221. https://doi.org/https://doi.org/10.1016/j.cej.2017.11.159

Kiernan, J., 2001. Classification and naming of dyes, stains and fluorochromes. Biotech.

Histochem. 76, 261–278. https://doi.org/10.1080/bih.76.5-6.261.278

Langmuir, I., 1918. THE ADSORPTION OF GASES ON PLANE SURFACES OF GLASS, MICA AND PLATINUM. J. Am. Chem. Soc. 40, 1361–1403. https://doi.org/10.1021/ja02242a004

Lin, J., Zhan, Y., 2012. Adsorption of humic acid from aqueous solution onto unmodified and surfactant-modified chitosan/zeolite composites. Chem. Eng. J. 200, 202–213.

Macioszek, V.K., Kononowicz, A.K., 2004. The evaluation of the genotoxicity of two commonly used food colors: Quinoline Yellow (E 104) and Brilliant Black BN (E 151). Cell. Mol. Biol. Lett. 9, 107–122.

Malik, P.K., 2004. Dye removal from wastewater using activated carbon developed from sawdust: Adsorption equilibrium and kinetics. J. Hazard. Mater. 113, 81–88. https://doi.org/10.1016/j.jhazmat.2004.05.022

Mezohegyi, G., van der Zee, F.P., Font, J., Fortuny, A., Fabregat, A., 2012. Towards advanced aqueous dye removal processes: A short review on the versatile role of activated carbon. J. Environ. Manage. 102, 148–164. https://doi.org/10.1016/j.jenvman.2012.02.021

Ng, C., Losso, J.N., Marshall, W.E., Rao, R.M., 2002. Freundlich adsorption isotherms of agricultural by-product-based powdered activated carbons in a geosmin–water system. Bioresour. Technol. 85, 131–135. https://doi.org/https://doi.org/10.1016/S0960-8524(02)00093-7

Nguyen, T.A., Juang, R.-S., 2013. Treatment of waters and wastewaters containing sulfur

dyes: A review. Chem. Eng. J. 219, 109–117. https://doi.org/https://doi.org/10.1016/j.cej.2012.12.102

Pan, Y., Wang, Y., Zhou, A., Wang, A., Wu, Z., Lv, L., Li, X., Zhang, K., Zhu, T., 2017. Removal of azo dye in an up-flow membrane-less bioelectrochemical system integrated with bio-contact oxidation reactor. Chem. Eng. J. 326, 454–461. https://doi.org/https://doi.org/10.1016/j.cej.2017.05.146

Patients, S., in Solid Cancer, P.C., Hassan, B.A.R., Yusoff, Z.B.M., Othman, M.A.H., Bin, S., information is available at the end of the Chapter, A., Http://dx.doi.org/10.5772/55358, 2012. We are IntechOpen , the world ' s leading publisher of Open Access books Built by scientists , for scientists TOP 1 %. Intech 13.

Peng, Y., Chen, D., Ji, J., Kong, Y., Huaixin, W., Yao, C., 2013. Chitosan-modified palygorskite: Preparation, characterization and reactive dye removal. Appl. Clay Sci. 74, 81–86.

Piccin, J.S., Dotto, G.L., Pinto, L.A.A., 2011. Adsorption isotherms and thermochemical data of FDandC RED N° 40 Binding by chitosan. Brazilian J. Chem. Eng. 28, 295–304. https://doi.org/10.1590/S0104-66322011000200014

Rafatullah, M., Sulaiman, O., Hashim, R., Ahmad, A., 2010. Adsorption of methylene blue on low-cost adsorbents: A review. J. Hazard. Mater. 177, 70–80. https://doi.org/https://doi.org/10.1016/j.jhazmat.2009.12.047

Riva, R., Ragelle, H., Des Rieux, A., Duhem, N., Jérôme, C., Préat, V., 2011. Chitosan and chitosan derivatives in drug delivery and tissue engineering. Adv. Polym. Sci. 244, 19–44. https://doi.org/10.1007/12_2011_137

Robinson, T., McMullan, G., Marchant, R., Nigam, P., 2001. Remediation of dyes in textile effluent: a critical review on current treatment technologies with a proposed alternative. Bioresour. Technol. 77, 247–255. https://doi.org/https://doi.org/10.1016/S0960-8524(00)00080-8

Rodríguez Couto, S., 2009. Dye removal by immobilised fungi. Biotechnol. Adv. 27, 227–235. https://doi.org/10.1016/j.biotechadv.2008.12.001

Seyed Dorraji, M.S., Mirmohseni, A., Carraro, M., Gross, S., Simone, S., Tasselli, F., Figoli, A., 2015. Fenton-like catalytic activity of wet-spun chitosan hollow fibers loaded with Fe3O4 nanoparticles: Batch and continuous flow investigations. J. Mol. Catal. A Chem. 398, 353–357. https://doi.org/https://doi.org/10.1016/j.molcata.2015.01.003

Sharma, P.K., Ayub, S., Tripathi, C.N., 2016. Isotherms describing physical adsorption of Cr(VI) from aqueous solution using various agricultural wastes as adsorbents. Cogent Eng. 3. https://doi.org/10.1080/23311916.2016.1186857

Tan, K.L., Hameed, B.H., 2017. Insight into the adsorption kinetics models for the removal of contaminants from aqueous solutions. J. Taiwan Inst. Chem. Eng. 74, 25–48. https://doi.org/https://doi.org/10.1016/j.jtice.2017.01.024

Tang, L., Yu, J., Pang, Y., Zeng, G., Deng, Y., Wang, J., Ren, X., Ye, S., Peng, B., Feng, H., 2018. Sustainable efficient adsorbent: Alkali-acid modified magnetic biochar derived from sewage sludge for aqueous organic contaminant removal, Chemical Engineering Journal. https://doi.org/10.1016/j.cej.2017.11.048

Temkin, M. and Pyzhev, V., 1940. Kinetics of the synthesis of ammonia on promoted iron catalysts. Acta Physicochim, 12(1), Pp.217-222.

Thinh, N.N., Hanh, P.T.B., Ha, L.T.T., Anh, L.N., Hoang, T.V., Hoang, V.D., Dang, L.H., Khoi, N. Van, Lam, T.D., 2013. Magnetic chitosan nanoparticles for removal of Cr(VI) from aqueous solution. Mater. Sci. Eng. C. Mater. Biol. Appl. 33, 1214–1218. https://doi.org/10.1016/j.msec.2012.12.013

Wang, J., Wang, Xiangxue, Zhao, G., Song, G., Chen, D., Chen, H., Xie, J., Hayat, T., Alsaedi, A., Wang, Xiangke, 2018. Polyvinylpyrrolidone and polyacrylamide intercalated molybdenum disulfide as adsorbents for enhanced removal of chromium(VI) from aqueous solutions. Chem. Eng. J. 334, 569–578. https://doi.org/https://doi.org/10.1016/j.cej.2017.10.068

Wang, Z., Xue, M., Huang, K., Liu, Z., 2011. 22395.Pdf. Adv. Treat. Text. Effl. 5.

Wawrzkiewicz, M., 2012. Anion Exchange Resins as Effective Sorbents for Acidic Dye Removal from Aqueous Solutions and Wastewaters. Solvent Extr. Ion Exch. 30, 507–523. https://doi.org/10.1080/07366299.2011.639253

Wittmar (geb. Barau), A., Böhler, H., Kayali, A., Ulbricht, M., 2020. One-step preparation of porous cellulose/chitosan macro-spheres from ionic liquid-based solutions. Cellulose 27. https://doi.org/10.1007/s10570-020-03165-y

Yagub, M., Sen, T., Afroze, S., Ang, H., 2014. Dye and Its Removal from Aqueous Solution by Adsorption: A Review. Adv. Colloid Interface Sci. 209. https://doi.org/10.1016/j.cis.2014.04.002

Zhao, R., Ma, T., Zhao, S., Rong, H., Tian, Y., Zhu, G., 2020. Uniform and stable immobilization of metal-organic frameworks into chitosan matrix for enhanced tetracycline removal from water. Chem. Eng. J. 382, 122893.

Raw data for calibration curve

The calibration curve was plotted based on the data below and displayed in Chapter 4

Table A. 1: Raw data for calibration curve

Concentration (mg/L)	Absorbance					
	Run					
	1	2	3	4	5	Average
25	0.4524	0.4508	0.4520	0.4516	0.4521	0.4518
50	0.9855	0.9848	0.9852	0.9855	0.9857	0.9853
75	1.3985	1.3986	1.3995	1.3989	1.3971	1.3985
100	1.7980	1.7980	1.7965	1.7980	1.8010	1.7983
125	2.3287	2.3348	2.3380	2.3410	2.3377	2.3360
150	2.7741	2.7563	2.7616	2.7389	2.7713	2.7604
175	3.1344	3.2985	3.2072	3.2112	3.0936	3.1890
200	3.5626	3.6245	3.4773	3.6118	3.6130	3.5778

A linear equation was obtained from the plotted data above and the equation is as below:

$$y = 0.018x \hspace{3cm} \text{[Equation A.1]}$$

where:

y is the absorbance

x is the concentration of BB dye left in mg/L

The linear plot shows the coefficient of determination is closed to unity with R^2 of 0.9989

Raw data for Experiment 1: The Effect of Adsorbent Dosage

Adsorbent dosage of 0.5 g

Table A. 2: Raw data for adsorbent dosage of 0.5 g

Time (min)	Absorbance						Concentration (mg/L)	Adsorption capacity, qe	Percentage of removal, R (%)
	Run								
	1	2	3	4	5	Average			
0	2.4601	2.4607	2.4609	2.4602	2.4603	2.4604	137.4547	0.0000	0.0000
10	2.4534	2.4361	2.4570	2.4506	2.4436	2.4481	136.7676	0.2061	0.4999
20	2.4369	2.4535	2.4434	2.4379	2.4358	2.4415	136.3966	0.3174	0.7698
30	2.4317	2.4282	2.4259	2.4383	2.4128	2.4274	135.6078	0.5541	1.3437
40	2.4094	2.4162	2.4159	2.4074	2.4219	2.4142	134.8693	0.7756	1.8810
50	2.3849	2.3945	2.3906	2.3947	2.4033	2.3936	133.7207	1.1202	2.7166
60	2.3915	2.3856	2.3647	2.3884	2.3835	2.3827	133.1140	1.3022	3.1580
120	2.3643	2.3730	2.3626	2.3776	2.3654	2.3686	132.3229	1.5396	3.7335
180	2.3655	2.3646	2.3575	2.3594	2.3703	2.3635	132.0369	1.6254	3.9416
240	2.2375	2.2475	2.2580	2.2406	2.2456	2.2458	125.4659	3.5966	8.7220
300	2.1254	2.1230	2.1258	2.1308	2.1241	2.1258	118.7609	5.6082	13.6000
1320	1.3192	1.3197	1.9187	1.3197	1.3200	1.4395	80.4168	17.1114	41.4958
1380	1.3805	1.3799	1.3793	1.3809	1.3807	1.3803	77.1095	18.1036	43.9019
1440	1.3084	1.3076	1.3074	1.3086	1.3088	1.3082	73.0816	19.3120	46.8323
2880	0.8111	0.8110	0.8112	0.8109	0.8107	0.8110	45.3061	27.6446	67.0392

Sample calculation

Calculation of concentrations BB dye left in the sample solution (mg/L)

By using Equation A.1, y = 0.018x

The concentration of BB dye left in the sample, $x = \dfrac{y}{0.018}$

For time 10 min, average absorbance, y = 2.4481

Therefore, the concentration of BB dye left, $x = \dfrac{2.4481}{0.018} = 137.4547$ mg/L

Calculation of percentage of removal, R (%)

By using Equation 3.1 in Chapter 3

$$\%R = \frac{C_0 - C_e}{C_0} \times 100\%$$ [Equation 3.1]

where:

C_e BB concentration at equilibrium (mg/L)

C_0 Initial BB concentration (mg/L)

At time 10 min, for adsorbent dosage of 0.5 g with BB solution volume is equal to 0.15 L

$$\%R = \frac{(137.4547 - 136.7676)}{137.4547} \times 100\% = 0.4999$$

Calculation of adsorption capacity, qe (mg/g)

By using Equation 3.2 in Chapter 3

$$q_e = \frac{(C_0 - C_e)V}{W}$$

[Equation 3.2]

where:

    q_e Adsorption capacity at equilibrium (mg/g)

    V   BB solution volume (L)

    W   Mass of adsorbent (g)

At time 10 min, for adsorbent dosage of 0.5 g with BB solution volume is equal to 0.15 L

$$q_e = \frac{(137.4547 - 136.7676)(0.15)}{0.5} = 0.2061 \text{ mg/g}$$

*Note: All calculations are made as the sample calculation for the other data including for other adsorbent dosage of 1.0 g, 1.5g, 2.0g and 2.5g as well as the initial dye concentration of 40 mg/L, 80 mg/L, 120 mg/L 160 mg/L and 200 mg/L

Adsorbent dosage of 1.0 g

Table A. 3: Raw data for adsorbent dosage of 1.0 g

Time (min)	Absorbance						Concentration (mg/L)	Adsorption capacity, qe	Percentage of removal, R (%)
	Run								
	1	2	3	4	5	Average			
0	2.4601	2.4607	2.4609	2.4602	2.4603	2.4604	137.4547	0.0000	0.0000
10	2.4481	2.4565	2.4468	2.4648	2.4784	2.4589	137.3698	0.0127	0.0618
20	2.4462	2.4522	2.4463	2.4506	2.4308	2.4452	136.6045	0.1275	0.6186
30	2.3429	2.3510	2.3526	2.3551	2.3545	2.3512	131.3531	0.9153	4.4390
40	2.3283	2.3457	2.3351	2.3391	2.3169	2.3330	130.3363	1.0678	5.1787
50	2.3372	2.3068	2.3199	2.3199	2.3217	2.3211	129.6704	1.1677	5.6632
60	2.3065	2.3087	2.3141	2.3195	2.3154	2.3128	129.2089	1.2369	5.9989
120	2.1994	2.1919	2.1938	2.1939	2.1921	2.1942	122.5821	2.2309	10.8200
180	2.1180	2.1123	2.1174	2.1093	2.1118	2.1138	118.0872	2.9051	14.0902
240	1.9296	1.9387	1.9407	1.9494	1.9383	1.9393	108.3430	4.3668	21.1791
300	1.8305	1.8302	1.8287	1.8333	1.8322	1.8310	102.2894	5.2748	25.5832
1320	0.8737	0.8732	0.8733	0.8737	0.8736	0.8735	48.7989	13.2984	64.4982
1380	0.7865	0.7864	0.7866	0.7862	0.7862	0.7864	43.9318	14.0284	68.0390
1440	0.7424	0.7422	0.7425	0.7421	0.7424	0.7423	41.4704	14.3977	69.8298
2880	0.3268	0.3269	0.3268	0.3267	0.3267	0.3268	18.2559	17.8798	86.7186

Adsorbent dosage of 1.5 g

Table A. 4: Raw data for adsorbent dosage of 1.5 g

Time (min)	Absorbance						Concentration (mg/L)	Adsorption capacity, qe	Percentage of removal, R (%)
	Run								
	1	2	3	4	5	Average			
0	2.4601	2.4607	2.4609	2.4602	2.4603	2.4604	137.4547	0.0000	0.0000
10	2.4360	2.4688	2.4418	2.4451	2.4506	2.4485	136.7855	0.0669	0.4869
20	2.3932	2.4000	2.4160	2.3994	2.4191	2.4055	134.3877	0.3067	2.2313
30	2.3691	2.3598	2.3553	2.3741	2.3500	2.3617	131.9358	0.5519	4.0151
40	2.3408	2.3333	2.3442	2.3280	2.3335	2.3360	130.5006	0.6954	5.0593
50	2.3305	2.3290	2.3422	2.3336	2.3371	2.3345	130.4179	0.7037	5.1194
60	2.3221	2.3218	2.3139	2.3321	2.3225	2.3225	129.7475	0.7707	5.6071
120	2.1802	2.1896	2.1832	2.1844	2.1895	2.1854	122.0883	1.5366	11.1793
180	1.9948	1.9919	2.0004	1.9986	1.9975	1.9966	111.5441	2.5911	18.8503
240	1.8011	1.7986	1.8040	1.8044	1.8020	1.8020	100.6715	3.6783	26.7603
300	1.5137	1.5149	1.5148	1.5161	1.5167	1.5152	84.6503	5.2804	38.4159
1320	0.8059	0.8055	0.8056	0.8056	0.8054	0.8056	45.0056	9.2449	67.2579
1380	0.7196	0.7196	0.7195	0.7195	0.7194	0.7195	40.1966	9.7258	70.7565
1440	0.7026	0.7028	0.7032	0.7034	0.7036	0.7031	39.2804	9.8174	71.4230
2880	0.2095	0.2094	0.2093	0.2091	0.2094	0.2093	11.6950	12.5760	91.4918

Adsorbent dosage of 2.0 g

Table A. 5: Raw data for adsorbent dosage of 2.0 g

Time (min)	Absorbance						Concentration (mg/L)	Adsorption capacity, qe	Percentage of removal, R (%)
	Run								
	1	2	3	4	5	Average			
0	2.4601	2.4607	2.4609	2.4602	2.4603	2.4604	137.4547	0.0000	0.0000
10	2.3885	2.3830	2.3765	2.3796	2.3749	2.3805	132.9888	0.3349	3.2490
20	2.3488	2.3491	2.3390	2.3317	2.3465	2.3430	130.8950	0.4920	4.7723
30	2.3215	2.3236	2.3116	2.3277	2.3152	2.3199	129.6045	0.5888	5.7112
40	2.2281	2.2369	2.2228	2.2281	2.2180	2.2268	124.4011	0.9790	9.4967
50	2.1746	2.1885	2.1894	2.1825	2.1779	2.1826	121.9318	1.1642	11.2931
60	2.1672	2.1649	2.1686	2.1635	2.1654	2.1659	121.0011	1.2340	11.9702
120	1.7881	1.7889	1.7875	1.7841	1.7869	1.7871	99.8380	2.8213	27.3666
180	1.7814	1.7789	1.7803	1.7802	1.7821	1.7806	99.4737	2.8486	27.6316
240	1.5649	1.5665	1.5659	1.5688	1.5661	1.5664	87.5106	3.7458	36.3350
300	1.4539	1.4525	1.4525	1.4530	1.4519	1.4528	81.1598	4.2221	40.9553
1320	0.8087	0.8092	0.8094	0.8097	0.8097	0.8093	45.2145	6.9180	67.1059
1380	0.6342	0.6348	0.6348	0.6351	0.6357	0.6349	35.4704	7.6488	74.1949
1440	0.6107	0.6103	0.6107	0.6107	0.6103	0.6105	34.1084	7.7510	75.1857
2880	0.1805	0.1805	0.1805	0.1806	0.1805	0.1805	10.0849	9.5527	92.6631

Adsorbent dosage of 2.5 g

Table A. 6: Raw data for adsorbent dosage of 2.5 g

Time (min)	Absorbance						Concentration (mg/L)	Adsorption capacity, qe	Percentage of removal, R (%)
	Run								
	1	2	3	4	5	Average			
0	2.4601	2.4607	2.4609	2.4602	2.4603	2.4604	137.4547	0.0000	0.0000
10	2.3682	2.3757	2.3717	2.3545	2.3689	2.3678	132.2793	0.3105	3.7652
20	2.3492	2.3420	2.3555	2.3472	2.3569	2.3502	131.2939	0.3697	4.4821
30	2.3384	2.3285	2.3233	2.3175	2.3166	2.3249	129.8804	0.4545	5.5104
40	2.2505	2.2434	2.2495	2.2253	2.2547	2.2447	125.4009	0.7232	8.7693
50	2.1903	2.1874	2.1915	2.1883	2.2017	2.1918	122.4492	0.9003	10.9167
60	2.1726	2.1658	2.1685	2.1642	2.1695	2.1681	121.1240	0.9798	11.8808
120	1.5648	1.5626	1.5646	1.5641	1.5627	1.5638	87.3609	3.0056	36.4439
180	1.5595	1.5585	1.5572	1.5628	1.5599	1.5596	87.1274	3.0196	36.6138
240	1.5424	1.5391	1.5403	1.5422	1.5435	1.5415	86.1173	3.0802	37.3486
300	1.3934	1.3950	1.3934	1.3927	1.3945	1.3938	77.8659	3.5753	43.3516
1320	0.6137	0.6134	0.6135	0.6136	0.6135	0.6135	34.2760	6.1907	75.0638
1380	0.5164	0.5165	0.5166	0.5165	0.5166	0.5165	28.8559	6.5159	79.0070
1440	0.5072	0.5073	0.5072	0.5071	0.5072	0.5072	28.3352	6.5472	79.3858
2880	0.1725	0.1724	0.1724	0.1726	0.1726	0.1725	9.6369	7.6691	92.9891

Raw data for Experiment 2: The Effect of Initial Dye Concentration

Initial dye concentration of 40 mg/L

Table A. 7: Raw data for initial dye concentration of 40 mg/L

Time (min)	Absorbance						Concentration (mg/L)	Adsorption capacity, qe	Percentage of removal, R (%)
	Run								
	1	2	3	4	5	Average			
0	0.8557	0.8553	0.8554	0.8557	0.8557	0.8556	47.7966	0.0000	0.0000
10	0.7795	0.7794	0.7792	0.7786	0.7778	0.7789	43.5140	0.2570	8.9602
20	0.7286	0.7286	0.7284	0.7282	0.7283	0.7284	40.6939	0.4262	14.8604
30	0.7288	0.7279	0.7280	0.7281	0.7279	0.7281	40.6782	0.4271	14.8932
40	0.7272	0.7271	0.7266	0.7276	0.7267	0.7270	40.6168	0.4308	15.0217
50	0.6915	0.6919	0.6921	0.6920	0.6923	0.6920	38.6570	0.5484	19.1220
60	0.6661	0.6659	0.6661	0.6661	0.6664	0.6661	37.2134	0.6350	22.1422
120	0.5370	0.5373	0.5369	0.5370	0.5372	0.5371	30.0045	1.0675	37.2247
180	0.5068	0.5081	0.5082	0.5081	0.5087	0.5080	28.3788	1.1651	40.6260
240	0.4476	0.4475	0.4474	0.4474	0.4474	0.4475	24.9978	1.3679	47.6998
300	0.3879	0.3879	0.3880	0.3880	0.3880	0.3880	21.6737	1.5674	54.6543
1320	0.0453	0.0452	0.0453	0.0454	0.0453	0.0453	2.5307	2.7160	94.7052
1380	0.0499	0.0499	0.0498	0.0499	0.0500	0.0499	2.7877	2.7005	94.1676
1440	0.0440	0.0438	0.0431	0.0429	0.0432	0.0434	2.4246	2.7223	94.9273
2880	0.0331	0.0331	0.0330	0.0330	0.0331	0.0331	1.8469	2.7570	96.1359

Initial dye concentration of 80 mg/L

Table A. 8: Raw data for initial dye concentration of 80 mg/L

Time (min)	Absorbance						Concentration (mg/L)	Adsorption capacity, qe	Percentage of removal, R (%)
	Run								
	1	2	3	4	5	Average			
0	1.5929	1.5907	1.5903	1.5904	1.5913	1.5911	88.8894	0.0000	0.0000
10	1.5761	1.5786	1.5797	1.5797	1.5787	1.5786	88.1877	0.0421	0.7894
20	1.5521	1.5536	1.5544	1.5567	1.5528	1.5539	86.8112	0.1247	2.3380
30	1.5487	1.5497	1.5501	1.5510	1.5510	1.5501	86.5978	0.1375	2.5781
40	1.5153	1.5174	1.5155	1.5162	1.5144	1.5158	84.6793	0.2526	4.7363
50	1.5115	1.5092	1.5114	1.5098	1.5098	1.5103	84.3765	0.2708	5.0769
60	1.4238	1.4229	1.4244	1.4246	1.4243	1.4240	79.5531	0.5602	10.5033
120	1.4179	1.4172	1.4164	1.4171	1.4183	1.4174	79.1832	0.5824	10.9194
180	1.3423	1.3431	1.3424	1.3440	1.3444	1.3432	75.0413	0.8309	15.5790
240	1.4474	1.1941	1.1933	1.1942	1.1942	1.2446	69.5330	1.1614	21.7759
300	1.1578	1.1578	1.1573	1.1579	1.1582	1.1578	64.6816	1.4525	27.2336
1320	0.2698	0.2697	0.2697	0.2698	0.2696	0.2697	15.0682	4.4293	83.0484
1380	0.2278	0.2277	0.2276	0.2278	0.2275	0.2277	12.7196	4.5702	85.6906
1440	0.1770	0.1770	0.1771	0.1769	0.1769	0.1770	9.8872	4.7401	88.8770
2880	0.0852	0.0853	0.0855	0.0854	0.0852	0.0853	4.7665	5.0474	94.6377

Initial dye concentration of 120 mg/L

Table A. 9: Raw data for initial dye concentration of 120 mg/L

| Time (min) | Absorbance | | | | | | Concentration (mg/L) | Adsorption capacity, qe | Percentage of removal, R (%) |
| | Run | | | | | | | | |
	1	2	3	4	5	Average			
0	2.4601	2.4607	2.4609	2.4602	2.4603	2.4604	137.4547	0.0000	0.0000
10	2.4360	2.4688	2.4418	2.4451	2.4506	2.4485	136.7855	0.0402	0.4869
20	2.3932	2.4000	2.4160	2.3994	2.4191	2.4055	134.3877	0.1840	2.2313
30	2.3691	2.3598	2.3553	2.3741	2.3500	2.3617	131.9358	0.3311	4.0151
40	2.3408	2.3333	2.3442	2.3280	2.3335	2.3360	130.5006	0.4173	5.0593
50	2.3305	2.3290	2.3422	2.3336	2.3371	2.3345	130.4179	0.4222	5.1194
60	2.3221	2.3218	2.3139	2.3321	2.3225	2.3225	129.7475	0.4624	5.6071
120	2.1802	2.1896	2.1832	2.1844	2.1895	2.1854	122.0883	0.9220	11.1793
180	1.9948	1.9919	2.0004	1.9986	1.9975	1.9966	111.5441	1.5546	18.8503
240	1.8011	1.7986	1.8040	1.8044	1.8020	1.8020	100.6715	2.2070	26.7603
300	1.5137	1.5149	1.5148	1.5161	1.5167	1.5152	84.6503	3.1683	38.4159
1320	0.8059	0.8055	0.8056	0.8056	0.8054	0.8056	45.0056	5.5469	67.2579
1380	0.7196	0.7196	0.7195	0.7195	0.7194	0.7195	40.1966	5.8355	70.7565
1440	0.7026	0.7028	0.7032	0.7034	0.7036	0.7031	39.2804	5.8905	71.4230
2880	0.2095	0.2094	0.2093	0.2091	0.2094	0.2093	11.6950	7.5456	91.4918

Initial dye concentration of 160 mg/L

Table A. 10: Raw data for initial dye concentration of 160 mg/L

Time (min)	Absorbance						Concentration (mg/L)	Adsorption capacity, qe	Percentage of removal, R (%)
	Run								
	1	2	3	4	5	Average			
0	3.1145	3.0746	3.0894	3.0735	3.0574	3.0819	172.1721	0.0000	0.0000
10	3.0831	3.0329	3.1351	3.0831	3.0329	3.0734	171.6994	0.0284	0.2745
20	3.0704	3.0808	3.0996	3.0190	3.0085	3.0557	170.7073	0.0879	0.8508
30	3.0605	3.0425	3.0555	3.0456	3.0311	3.0470	170.2257	0.1168	1.1305
40	3.0841	3.0222	3.0040	3.0262	3.0753	3.0424	169.9642	0.1325	1.2823
50	2.8987	3.0304	3.0398	3.0016	2.9889	2.9979	167.4804	0.2815	2.7250
60	3.0304	2.9501	2.8881	2.9424	2.8647	2.9328	163.8436	0.4997	4.8373
120	2.9501	2.8987	2.8544	2.8496	2.9128	2.8732	160.5140	0.6995	6.7712
180	2.7771	2.8340	2.7632	2.7819	2.7864	2.7885	155.7832	0.9833	9.5189
240	2.5776	2.5852	2.5687	2.5702	2.5660	2.5735	143.7732	1.7039	16.4945
300	1.1934	2.7460	2.7579	2.7769	2.7376	2.4424	136.4447	2.1436	20.7510
1320	1.1149	1.1141	1.1139	1.1141	1.1139	1.1142	62.2447	6.5956	63.8474
1380	0.9304	0.9299	0.9304	0.9300	0.9299	0.9301	51.9620	7.2126	69.8197
1440	0.7572	0.7275	0.7574	0.7577	0.7578	0.7515	41.9844	7.8113	75.6149
2880	0.2706	0.2706	0.2705	0.2708	0.2707	0.2706	15.1196	9.4232	91.2183

Initial dye concentration of 200 mg/L

Table A. 11: Raw data for initial dye concentration of 200 mg/L

Time (min)	Absorbance						Concentration (mg/L)	Adsorption capacity, qe	Percentage of removal, R (%)
	Run								
	1	2	3	4	5	Average			
0	3.8934	3.8809	3.8277	3.7775	3.7179	3.8195	213.3788	0.0000	0.0000
10	3.8100	3.8348	3.9488	3.7831	3.6320	3.8017	212.3877	0.0595	0.4645
20	3.8251	3.8278	3.8555	3.7591	3.7344	3.8004	212.3117	0.0640	0.5001
30	3.9309	3.5779	3.6573	3.9332	3.8558	3.7910	211.7883	0.0954	0.7454
40	3.7351	3.7485	3.6900	3.7338	3.7473	3.7309	208.4324	0.2968	2.3181
50	3.3880	3.5699	3.7581	3.6691	3.7871	3.6344	203.0413	0.6202	4.8446
60	3.6126	3.6668	3.4300	3.8428	3.4711	3.6047	201.3777	0.7201	5.6243
120	3.4976	3.5229	3.6678	3.5472	3.5910	3.5653	199.1788	0.8520	6.6548
180	3.7513	3.5136	3.4369	3.5420	3.5377	3.5563	198.6760	0.8822	6.8905
240	3.4454	3.3813	3.3662	3.4340	3.4356	3.4125	190.6425	1.3642	10.6554
300	3.1433	3.1449	3.1212	3.2045	3.3337	3.1895	178.1855	2.1116	16.4933
1320	1.4332	1.4355	1.4343	1.4323	1.4294	1.4329	80.0525	7.9996	62.4834
1380	1.1891	1.1904	1.1907	1.1917	1.1901	1.1904	66.5028	8.8126	68.8335
1440	1.0787	1.0782	1.0782	1.0781	1.0784	1.0783	60.2413	9.1882	71.7679
2880	0.4517	0.4519	0.4519	0.4515	0.4516	0.4517	25.2358	11.2886	88.1733

Raw data for Experiment 3: Chitosan/ Activated Carbon Composite Adsorbent

Adsorbent dosage of 0.5 g with initial dye concentration of 40 mg/L

Table A. 12: Raw data for chitosan/activated carbon composite adsorbent

Time (min)	Absorbance						Concentration (mg/L)	Adsorption capacity, qe	Percentage of removal, R (%)
	Run								
	1	2	3	4	5	Average			
0	0.8051	0.8055	0.8053	0.8051	0.8051	0.8052	44.9844	0.0000	0.0000
10	0.7801	0.7802	0.7802	0.7801	0.7805	0.7802	43.5877	0.0838	3.1047
20	0.7787	0.7787	0.7788	0.7790	0.7794	0.7789	43.5151	0.0882	3.2662
30	0.7717	0.7708	0.7712	0.7709	0.7709	0.7711	43.0782	0.1144	4.2374
40	0.7634	0.7633	0.7630	0.7629	0.7628	0.7631	42.6302	0.1413	5.2334
50	0.7565	0.7564	0.7565	0.7569	0.7564	0.7565	42.2648	0.1632	6.0456
60	0.7530	0.7525	0.7527	0.7527	0.7525	0.7527	42.0492	0.1761	6.5249
120	0.6021	0.6019	0.6017	0.6018	0.6018	0.6019	33.6235	0.6817	25.2552
180	0.4826	0.4815	0.4816	0.4818	0.4819	0.4819	26.9207	1.0838	40.1555
240	0.4501	0.4501	0.4503	0.4501	0.4501	0.4501	25.1475	1.1902	44.0973
300	0.3912	0.3933	0.3903	0.3933	0.3915	0.3919	21.8950	1.3854	51.3276
1320	0.0450	0.0449	0.0449	0.0449	0.0448	0.0449	2.5084	2.5486	94.4239
1380	0.0340	0.0339	0.0339	0.0339	0.0338	0.0339	1.8939	2.5854	95.7900
1440	0.0301	0.0301	0.0302	0.0303	0.0302	0.0302	1.6860	2.5979	96.2520
2880	0.0228	0.0227	0.0227	0.0227	0.0228	0.0227	1.2704	2.6228	97.1759

Raw data for adsorption isotherms

Raw data for adsorption isotherms model for chitosan adsorbent film at optimum condition of 0.5 g adsorbent dosage and 40 mg/L of initial dye concentration

Table A. 13: Adsorption isotherms raw data for chitosan adsorbent films

Langmuir		Freundlich		Temkin	
Y	X	Y	X	Y	X
1/qe	1/Ce	log qe	log Ce	qe	ln Ce
3.8916	0.0230	-0.5901	1.63863	0.2570	3.7731
2.3465	0.0246	-0.3704	1.60953	0.4262	3.7061
2.3413	0.0246	-0.3695	1.60936	0.4271	3.7057
2.3213	0.0246	-0.3657	1.60871	0.4308	3.7042
1.8236	0.0259	-0.2609	1.58723	0.5484	3.6547
1.5748	0.0269	-0.1972	1.5707	0.6350	3.6167
0.9367	0.0333	0.0284	1.47719	1.0675	3.4013
0.8583	0.0352	0.0664	1.45299	1.1651	3.3456
0.7310	0.0400	0.1361	1.3979	1.3679	3.2188
0.6380	0.0461	0.1952	1.33593	1.5674	3.0761
0.3682	0.3951	0.4339	0.40325	2.7160	0.9285
0.3703	0.3587	0.4315	0.44525	2.7005	1.0252
0.3673	0.4124	0.4349	0.38464	2.7223	0.8857
0.3627	0.5414	0.4404	0.26645	2.7570	0.6135

Raw data for adsorption isotherms model for chitosan/activated carbon adsorbent films at optimum condition of 0.5 g adsorbent dosage and 40 mg/L of initial dye concentration

Table A. 14: Adsorption isotherms raw data for chitosan/activated carbon adsorbent films

Langmuir		Freundlich		Temkin	
Y	X	Y	X	Y	X
1/qe	1/Ce	log qe	log Ce	qe	ln Ce
11.9333	0.0229	-1.0768	1.63936	0.0838	3.7748
11.3435	0.0230	-1.0547	1.63864	0.0882	3.7731
8.7436	0.0232	-0.9417	1.63426	0.1144	3.7630
7.0796	0.0235	-0.8500	1.62972	0.1413	3.7526
6.1285	0.0237	-0.7874	1.62598	0.1632	3.7440
5.6782	0.0238	-0.7542	1.62376	0.1761	3.7388
1.4670	0.0297	-0.1664	1.52664	0.6817	3.5152
0.9227	0.0371	0.0350	1.43009	1.0838	3.2929
0.8402	0.0398	0.0756	1.40049	1.1902	3.2248
0.7218	0.0457	0.1416	1.34034	1.3854	3.0863
0.3924	0.3987	0.4063	0.39939	2.5486	0.9196
0.3868	0.5280	0.4125	0.27735	2.5854	0.6386
0.3849	0.5931	0.4146	0.22687	2.5979	0.5224
0.3813	0.7872	0.4188	0.10394	2.6228	0.2393

Raw data for adsorption kinetics

Pseudo-first-order kinetic model

Raw data for Pseudo-first-order kinetic model for chitosan and chitosan/activated carbon adsorbent films

Table A. 15: Raw data for Pseudo-first-order kinetic model

Chitosan		Chitosan/activated carbon	
Y	X	Y	X
ln(qe-qt)	t (hr)	ln(qe-qt)	t (hr)
1.0141	0.00	0.9643	0.00
0.9163	0.17	0.9318	0.17
0.8462	0.33	0.9301	0.33
0.8458	0.50	0.9197	0.50
0.8442	0.67	0.9089	0.67
0.7924	0.83	0.9000	0.83
0.7524	1.00	0.8948	1.00
0.5244	2.00	0.6633	2.00
0.4649	3.00	0.4311	3.00
0.3286	4.00	0.3595	4.00
0.1736	5.00	0.2131	5.00
-3.1935	22.00	-2.5999	22.00
-2.8745	23.00	-3.2859	23.00
-3.3622	24.00	-3.6913	24.00

Pseudo-second-order kinetic model

Raw data for Pseudo-second-order kinetic model for chitosan and chitosan/activated carbon adsorbent films

Table A. 16: Raw data for Pseudo-second-order kinetic model

Chitosan		Chitosan/ activated carbon	
t/qt	t (hr)	t/qt	t (hr)
Y	X	Y	X
0.6486	0.17	1.9889	0.17
0.7822	0.33	3.7812	0.33
1.1707	0.50	4.3718	0.50
1.5475	0.67	4.7197	0.67
1.5196	0.83	5.1070	0.83
1.5748	1.00	5.6782	1.00
1.8735	2.00	2.9340	2.00
2.5749	3.00	2.7680	3.00
2.9241	4.00	3.3607	4.00
3.1900	5.00	3.6092	5.00
8.1003	22.00	8.6323	22.00
8.5168	23.00	8.8960	23.00
8.8160	24.00	9.2382	24.00